

学位論文

Studies on Rab5 effectors in *Arabidopsis thaliana*

(シロイヌナズナにおける Rab5 エフェクターの研究)

平成 28 年 7 月博士 (理学) 申請

東京大学大学院理学系研究科

生物科学専攻

桜井 一

Abstract

RAB5 GTPases act as molecular switches that regulate various endosomal functions in animal cells, including homotypic fusion of early endosomes, endosomal motility, endosomal signaling, and subcompartmentalization of the endosomal membrane. RAB5 proteins fulfill these diverse functions through interactions with downstream effector molecules. Two canonical RAB5 members, ARA7 and RAB HOMOLOG1 (RHA1), are encoded in the *Arabidopsis thaliana* genome. ARA7 and RHA1 play crucial roles in endocytic and vacuolar trafficking pathways. Plant RAB5 GTPases function via interactions with effector molecules, whose identities and functions are currently unclear. In this thesis, I searched for canonical RAB5 effector molecules of *A. thaliana* and identified a candidate, which I called ENDOSOMAL RAB EFFECTOR WITH PX-DOMAIN (EREX). The intimate genetic interaction between *EREX* and *RAB5* members, the results from subcellular colocalization experiments, and the direct interaction observed in an *in vitro* pull-down assay strongly suggest that *EREX* is a genuine effector of canonical RAB5s in *A. thaliana*. I further found that close homologs of *EREX* play partially redundant functions with *EREX* in the transport of seed storage proteins. My results indicate that canonical plant RAB5s acquired distinct effector molecules from those of non-plant systems to fulfill their functions.

Abbreviations

EREX	endosomal Rab effector with PX-domain
EREL	EREX-like
GEF	guanine nucleotide exchange factor
PI	phosphatidylinositol
VPS9a	vacuolar protein sorting 9a
TGN	<i>trans</i> -Golgi network
PSV	protein storage vacuole
CT24	24 C-terminal amino acids of α' -subunit of β -conglycinin

Table of Contents

Chapter 1: Introduction	1
Chapter 2: Results	8
2.1 Screening for Proteins That Interact with Canonical RAB5	
2.2 Interaction of EREX with Canonical RAB5	
2.3 EREX Depends on RAB5 Activity to Localize to Endosomes	
2.4 Characterization of <i>erex</i> and <i>erel</i> Mutants	
2.5 Expression and Subcellular Localization of EREX in Plants	
2.6 RAB5 Acts Upstream of EREX	
2.7 EREX and EREL1 Are Required for the Vacuolar Transport of Storage Proteins	
Chapter 3: Discussion	39
3.1 Redundant Functions of EREX and EREL1 and 2	
3.2 Structural Features of EREX/EREL Members	
3.3 How Does EREX Mediate Vacuolar Trafficking with RAB5?	
3.4 Concluding Remarks	
Experimental Procedures	50
Accession Numbers	57
Acknowledgements	58
References	59

Chapter 1: Introduction

Eukaryotic cells utilize various membrane-bound organelles, each of which comprises a specific set of proteins and lipids to fulfill distinctive functions. The endosome is one of the single membrane bound organelles and classically categorized into three subpopulations according to their functions in endocytosis. First, early endosomes (EEs) are generated by fusion of endocytic vesicles derived from the invaginated plasma membrane (PM), which internalize extracellular elements and integral proteins residing in the PM. Then, recycling endosomes operate as a sorting center, where the cargos from EEs are sorted into ones for late endosomes (LEs) for degradation and others for the PM to be recycled. LEs contain intraluminal vesicles (ILVs) formed through the action of endosomal sorting complexes required for transport (ESCRT), thus referred to as multivesicular endosomes (MVEs). This structure allows transmembrane proteins to be enclosed inside MVEs and degraded completely by fusion with lysosomes/vacuoles. This functional transition of endosomes is achieved via alteration in nature and/or morphology of the endosomal membrane including fission/fusion, tubulation, and maturation, all of which are tightly correlated with functions of small GTPases. ARF and RAB GTPases are small GTPases that participate in regulation of endosomal membrane trafficking; for instance, in animal cells, ARF6 acts in endocytosis from the PM, RAB5 promotes tethering between EEs and promotes the homotypic fusion, RAB11 organizes tubular structures for retrograde transport. It is also shown that RAB5 converts the endosomal membrane components to mature to

RAB7-residing LEs (D'Souza-Schorey and Chavrier, 2006; Simonsen et al., 1998; Nielsen et al., 2000; Hsu and Prekeris, 2010; Epp et al., 2011). Studies of these small GTPases have contributed to resolve the mechanism of the complicated endocytic network.

Endosomal trafficking plays pivotal roles in various cellular functions in animals and plants, which include the maintenance of cell polarity, selective degradation and recycling of membrane proteins, and nutrient utilization (Jolliffe et al., 2005; Miao et al., 2008; Grant and Donaldson, 2009; Friml, 2010; Reyes et al., 2011; Contento and Bassham, 2012). RAB GTPases act as molecular switches by cycling between GTP-bound active and GDP-bound inactive states, serving as key regulators of membrane trafficking, including endosomal trafficking (Saito and Ueda, 2009). When RAB GTPases are activated by the replacement of GDP with GTP, which is mediated by guanine nucleotide exchange factors (GEFs), they interact with specific sets of interacting partners collectively called RAB effectors. Through their interaction with effector molecules, RAB GTPases evoke a wide spectrum of downstream events, including the tethering of transport vesicles to target organelles, the formation of subdomains on organelle membranes, organelle movement, alteration of lipid composition in organelle membranes, and organelle maturation (Stenmark, 2009; Mizuno-Yamasaki et al., 2012). Once GTP is hydrolyzed by the action of GTPase activating proteins, the GDP-bound RAB proteins are detached from the membranes by forming complexes with GDP dissociation inhibitors and are retained in the cytosol

until the next round of the GTPase cycle (Seabra and Wasmeier, 2004; Goody et al., 2005).

RAB5 is one of the best-characterized groups of RAB proteins in animal systems (Somsel Rodman and Wandinger-Ness, 2000; Benmerah, 2004; Galvez et al., 2012). Animal RAB5s interact with more than 20 proteins in the GTP-bound state (Christoforidis and Zerial, 2000), including class I and class III phosphatidylinositol-3 kinases and phosphoinositide phosphatases (Christoforidis et al., 1999; Shin et al., 2005). Phosphoinositides are a minor group of glycerophospholipids, which are largely conserved as endosomal membrane components. Phosphatidylinositol (PI) is biosynthesized at the ER and consists of fatty acids and an inositol ring, of which 3-, 4-, and 5-positions are exposed to phosphorylation. Therefore, seven variations (only six variations were found in plants) of phosphoinositides are synthesized by a variety of kinases and phosphatases, which play important roles in membrane trafficking with binding-partner proteins (Jean and Kiger, 2012). Indeed, various proteins with phosphoinositide-binding moieties such as Early Endosome Antigen1 (EEA1), Rabenosyn-5, Rabankyrin-5, and APPL1 and 2, which shuttle between the endosomal membrane and nucleus, have also been identified as RAB5 effectors (Simonsen et al., 1998; Nielsen et al., 2000; Miaczynska et al., 2004; Schnatwinkel et al., 2004). These lines of evidence strongly suggest that there is a tight correlation between RAB5 function and phosphoinositides in animal cells.

RAB GTPases also play key roles in membrane trafficking pathways in plant

cells (Lycett, 2008; Nielsen et al., 2008; Pedrazzini et al., 2013). The *Arabidopsis thaliana* genome encodes 57 RAB GTPases, which are classified into 8 subgroups according to their similarity to animal Rab GTPases (Woollard and Moore, 2008). Among these subgroups, the RAB5 group (also called RABF) consists of three members, which are further classified into two subtypes: plant-unique ARA6 (also known as RABF1) and the canonical RAB5 group (ARA7 and RAB HOMOLOG1 [RHA1], also known as RABF2b and RABF2a, respectively) (Ueda et al., 2001; Ueda et al., 2004; Ebine and Ueda, 2008). Despite the differences in their primary structures, these RAB5 members are activated by the same GEF, VACUOLAR PROTEIN SORTING 9a (VPS9a), whose loss of function results in embryonic lethality (Goh et al., 2007; Uejima et al., 2010; Uejima et al., 2013). The double mutant of canonical RAB5, *ara7 rha1*, also exhibits gametophytic lethality (Dhonukshe, 2009). These lines of evidence indicate that RAB5 GTPases fulfill an essential function in *Arabidopsis*, although the molecular basis underlying this function remains mostly unknown.

Analyzing plant RAB5 effectors is an effective approach for unraveling the molecular mechanisms of RAB5-mediated membrane trafficking. However, clear homologs of animal RAB5 effectors such as Rabaptin-5 (Stenmark et al., 1995) and EEA1 (Simonsen et al., 1998) are not found in plants, suggesting that the operation of RAB5-dependent membrane trafficking in plants is distinct from that in non-plant systems. The unique mechanism of the RAB5-mediated trafficking pathway is also highlighted by the divergent functions of the two RAB5 subtypes in plants. Canonical

RAB5 and ARA6 are localized to distinct but overlapping populations of MVEs (Ueda et al., 2004; Haas et al., 2007; Ebine et al., 2011), suggesting diversification of their functions. ARA6 acts in the endosome-to-plasma membrane trafficking pathway (Ebine et al., 2011) and may also be involved in a vacuolar trafficking pathway (Bottanelli et al., 2011). ARA7 and RHA1, in contrast, redundantly regulate endocytic and vacuolar trafficking pathways (Sohn et al., 2003; Kotzer et al., 2004; Dhonukshe et al., 2006; Ebine et al., 2011; Beck et al., 2012; Ebine et al., 2014). The unique organization of endosomal trafficking in plants is also demonstrated by the observation that the *trans*-Golgi network (TGN) acts as an early endosome in plants (Dettmer, 2006; Lam et al., 2007; Viotti et al., 2010), from which MVEs are proposed to be directly generated by maturation (Niemes et al., 2010; Scheuring et al., 2011). The RAB11 group (also known as RABA in Arabidopsis), which is localized to TGN-related secretory compartments and is involved in cell plate formation and tip growth (Preuss et al., 2004; Chow et al., 2008; Szumlanski and Nielsen, 2009; Kang et al., 2011; Asaoka et al., 2012; Feraru et al., 2012; Berson et al., 2014; Kirchhelle et al., 2016), is also implicated in endosomal/vacuolar trafficking (Bottanelli et al., 2011; Choi et al., 2013). These lines of evidence indicate that endosomal trafficking in plant cells operates in a different manner from that in non-plant organisms.

There are several reports on the effectors of plant RAB GTPases, one of which is PI-4K β 1, a class III phosphatidylinositol-4 kinase, identified as an effector of Rab11/RabA4b regulating polarized expansion of root hair cells (Preuss et al., 2006).

Moreover, PIP5K2, which is a class I phosphatidylinositol-4-phosphate 5-kinase, is reported as an effector of Rab8/RabE1d (Camacho et al., 2009). These findings also implied close relationships between RAB GTPases and phosphoinositides in plants. Interestingly, although PI-4K β 1 is identified as an effector of RAB11 in animal, PIP5K2 is claimed as a RAB8 effector only in plants (Zerial and McBride, 2001; de Graaf et al., 2004). Vps34/vps15 is a class III phosphatidylinositol-3 kinase complex and an effector of RAB5 in animal. In contrast, the kinase complex has not been shown to bind to RAB5s in plants (Christoforidis et al., 1999; Itoh and Sakurai, unpublished). Differentiation of the binding properties of these kinases are also reminiscent of the diversity of endosomal trafficking between animals and plants.

Recently, a complex consisting of SAND/MONENSIN SENSITIVITY1 (MON1) and CALCIUM CAFFEINE ZINC SENSITIVITY1 (CCZ1) was demonstrated to act as an effector of canonical plant RAB5 (Cui et al., 2014; Ebine et al., 2014; Singh et al., 2014). The SAND-CCZ1 complex interacts with GTP-bound RAB5 and serves as a GEF for RAB7, which leads to RAB5-to-RAB7 conversion on the endosome. This finding clearly demonstrates that plants harbor an endosomal/vacuolar trafficking pathway in which RAB5 and RAB7 act sequentially, as proposed previously (Bottanelli et al., 2012). In addition to this pathway, plants are also equipped with at least two distinct trafficking pathways for vacuoles, which are distinctly dependent on RAB5 and RAB7 (Bottanelli et al., 2011; Ebine et al., 2014). This complexity in the vacuolar trafficking system also indicates that plants have evolved elaborate endosomal

trafficking pathways in a unique manner.

To begin characterizing the roles of canonical plant RAB5 in the endosomal trafficking pathways, I carried out yeast two-hybrid screening for interacting partners of canonical RAB5 from *Arabidopsis*. I isolated an interacting partner of RAB5 that harbors a phosphoinositide-binding domain. My results indicate that this protein acts as a RAB5 effector and mediates vacuolar trafficking of seed storage proteins by interacting with canonical RAB5.

Chapter 2: Results

2.1 Screening for proteins that interact with canonical RAB5

To identify candidates for effectors of canonical RAB5 in Arabidopsis, I carried out yeast two-hybrid screening using constitutively active ARA7 (ARA7^{Q69L}) as bait. In this study, C-terminal cysteine residues of RAB GTPases were deleted to ensure their nuclear localization in yeast cells. I screened a cDNA library prepared from 4-day-old Arabidopsis root tissues and identified a positive clone containing a partial sequence of cDNA for *At3g15920*, which encodes a partial protein lacking the N-terminal 27 amino acids of the predicted full-length protein (Figure 1A). This candidate protein exhibited a positive interaction with the other Arabidopsis canonical RAB5, RHA1, but did not interact with constitutively active mutants of RAB7/RABG3b, RAB11/RABA1e, or ARA6/RABF1 (Figure 1A). Thus, the identified candidate protein specifically interacted with canonical RAB5. *At3g15920* encodes a protein of unknown function, which contains a phox homology (PX) domain known as a phosphoinositide-binding module. I named this protein ENDOSOMAL RAB EFFECTOR WITH PX-DOMAIN (EREX) and investigated the possibility that this protein acts as an effector of canonical RAB5. There are 11 genes encoding PX domain-containing proteins in the Arabidopsis genome, which are classified into 4 subgroups (van Leeuwen et al., 2004). Among these genes, *At4g32160* and *At2g25350* encode structurally similar proteins to EREX, which I named EREX-LIKE1 (EREL1) and EREL2, respectively. I isolated ORF sequences for full-length EREX and EREL proteins and used the yeast two-hybrid method to

determine whether they interacted with RAB5. Full-length EREX also interacted with wild-type and constitutively active ARA7 and RHA1. In contrast, an interaction between EREL proteins and RAB GTPases was not detected by this method (Figure 1B).

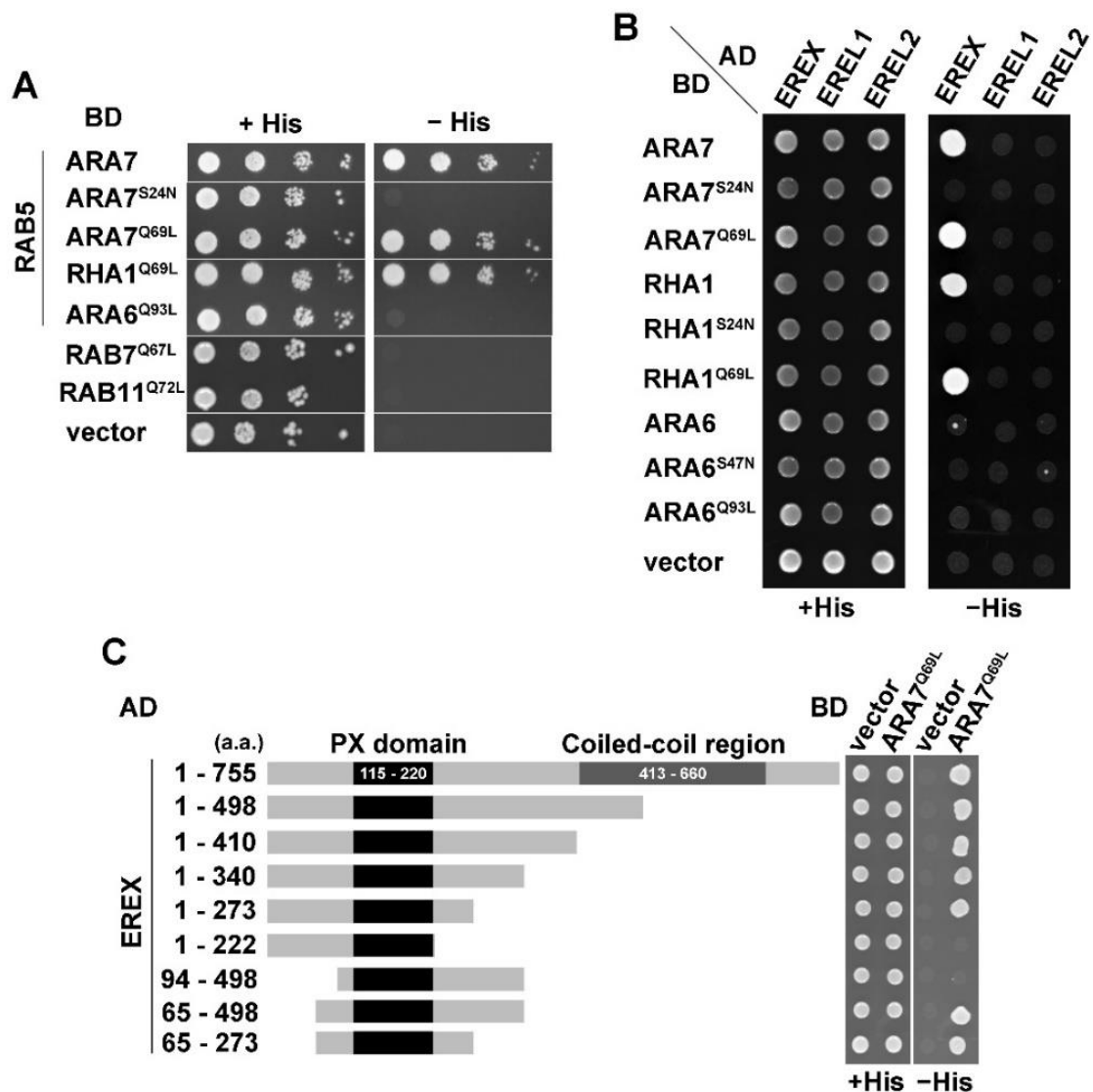


Figure 1. Interaction of EREX and EREL members with RAB GTPases detected by the yeast two-hybrid method

(A-C) RAB proteins were expressed as fusion proteins with a DNA binding domain (BD). EREX and EREL members were expressed as fusions with a transcriptional activation domain (AD). Interactions between the two cotransformed proteins were tested using the *HIS3* reporter gene in the AH109 yeast strain. Cells were spotted on synthetic medium lacking tryptophan and leucine (+His) or lacking tryptophan, leucine, and histidine (-His) and incubated at 30°C for 5 days. (A) The originally isolated plasmid containing a partial sequence of cDNA for EREX was re-transformed with the plasmids containing endosomal RABs with the GTP-freeze (Q-to-L mutations) or GDP-freeze (S-to-N mutation) mutations. The result of a ten-fold serial dilution is indicated. (B) EREX, EREL1, and EREL2 were fused to the AD and cotransformed with BD-ARA7, BD-RHA1, and BD-ARA6 containing the indicated mutations. (C) Deletion mutants of EREX were cotransformed with constitutively active ARA7.

2.2 Interaction of EREX with canonical RAB5

To determine the region of EREX responsible for the interaction with RAB5, I constructed a deletion series of EREX and examined the interaction with constitutively active ARA7. I identified the polypeptide containing amino acids 65–273 of EREX (EREX⁶⁵⁻²⁷³) as the minimum region required for the interaction with ARA7 (Figure 1C). Thus, the PX domain and its flanking regions are responsible for interaction with RAB5, and the coiled-coil region is dispensable for this interaction.

I then attempted to detect direct interaction between EREX and ARA7 with an *in vitro* pull-down assay using bacterially expressed and purified proteins. At first, I used the full-length EREX protein tagged with glutathione S-transferase (GST) for the assay, but I could not detect its binding with ARA7 because the full-length EREX protein was easily degraded during the experimental procedure. I then examined the interaction with GST-tagged EREX⁶⁵⁻²⁷³. I incubated GST-EREX⁶⁵⁻²⁷³ with His₆-tagged ARA7 or ARA6 in the presence of GTP γ S and examined whether these RAB proteins were pulled down using glutathione sepharose. As suggested from the results of the yeast two-hybrid assay, GST-EREX⁶⁵⁻²⁷³ pulled down ARA7-His₆ but not ARA6-His₆ (Figure 2A). I confirmed that GST alone did not pull down ARA7-His₆. When GTP γ S in the binding buffer was replaced with GDP, the amount of ARA7-His₆ pulled down by GST-EREX⁶⁵⁻²⁷³ was drastically reduced (Figure 2B). These results further indicate that canonical RAB5 interacts with EREX in the GTP-bound active state.

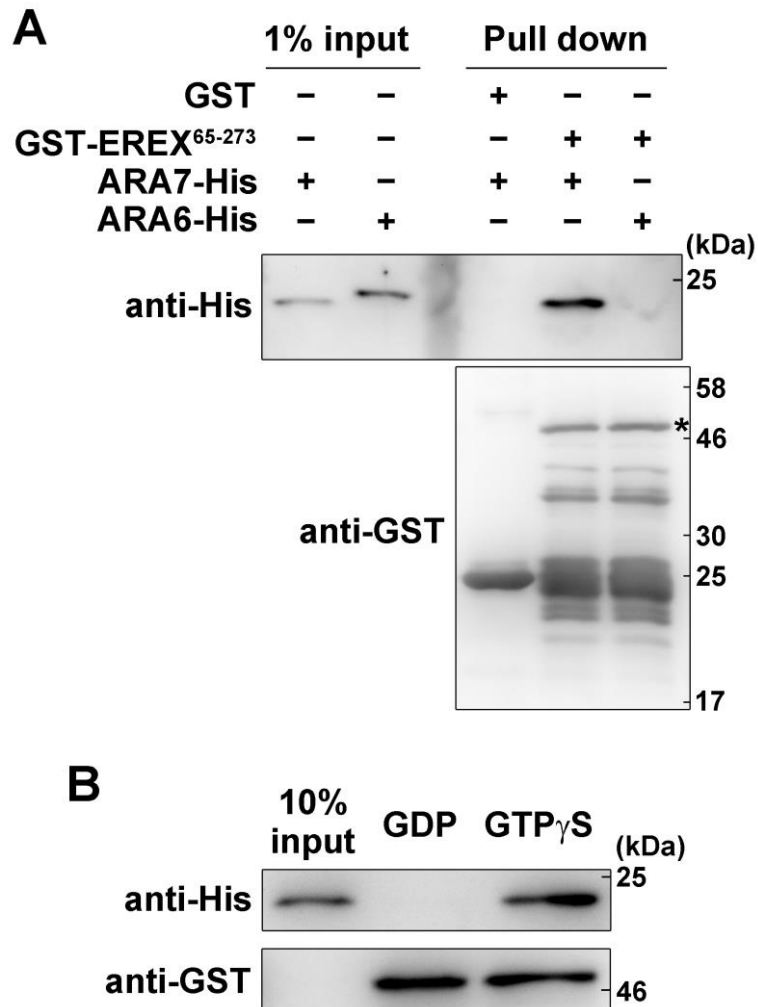


Figure 2. Interactions between EREX⁶⁵⁻²⁷³ and ARA7 detected in the *in vitro* pull-down assay

(A) The interaction between GST-tagged EREX⁶⁵⁻²⁷³ and His₆-tagged ARA7 or ARA6 was tested in the presence of 10 μ M GTP γ S. Proteins were precipitated using Glutathione-Sepharose 4B resin and analyzed by immunoblotting using anti-His₆ antibody and anti-GST antibodies. EREX⁶⁵⁻²⁷³ specifically and directly interacted with ARA7. Although anti-GST antibodies detected intact molecular weight of GST-EREX⁶⁵⁻²⁷³ (asterisk), there were a number of additional detections suggested the nature of EREX proteins as an easily degradation. (B) GST-EREX⁶⁵⁻²⁷³ and ARA7-His₆ were incubated with Glutathione-Sepharose 4B resin in the presence of 25 μ M GTP γ S or GDP. GST-EREX⁶⁵⁻²⁷³ interacted with GTP γ S-bound ARA7.

2.3 EREX depends on RAB5 activity to localize to endosomes

I then analyzed the subcellular localization of N-terminally green fluorescent protein (GFP)-tagged EREX in the protoplasts of suspension-cultured Arabidopsis cells. When GFP-EREX was expressed alone under the control of the CaMV35S promoter, fluorescence from GFP-EREX was predominantly observed in the cytosol and rarely localized to punctate structures (Figure 3A). When EREX was coexpressed with ARA7, EREX was targeted to the punctate compartments and colocalized with ARA7 (Figure 3B). In contrast, a similar effect on GFP-EREX was not observed for RABG3b, a member of the RAB7 group (Figure 4A). I then examined whether the nucleotide states of ARA7 affected the localization of GFP-EREX. When coexpressed with a GDP-fixed mutant of ARA7 (ARA7^{S24N}) tagged with Venus, EREX dispersed into the cytosol (Figure 3B). Conversely, when coexpressed with GTP-fixed ARA7^{Q69L}, which was localized to the punctate compartments and the vacuolar membrane, GFP-EREX was also targeted to the same puncta and the vacuolar membrane (Figure 4A). GTP-fixed ARA6^{Q93L}, which was also localized to the punctate compartments and the vacuolar membrane, had no effect on GFP-EREX (Figure 4A). Thus, the endosomal localization of EREX depends on the activating state of ARA7, which suggests that EREX and canonical RAB5 actually act together in plant cells. This result was further supported by quantitative analysis. When GFP-EREX was coexpressed with wild-type ARA7, 22.6 ± 7.2 punctate structures were observed in a confocal section of a protoplast, whereas 2.33 ± 2.9 puncta of GFP-EREX were observed when GFP-EREX was expressed alone

(Figure 3C). Only 0.111 ± 0.32 GFP-EREX-positive dots were observed when GFP-EREX was coexpressed with ARA7^{S24N}. Coexpression of VAMP727, a soluble N-ethylmaleimide-sensitive factor attachment protein receptor (SNARE) that resides on the endosome with canonical RAB5 (Ueda et al., 2004; Ebine et al., 2008), did not affect the subcellular localization of GFP-EREX (1.86 ± 2.3 puncta were observed in a confocal section of a protoplast). These results indicate that EREX is specifically recruited to endosomes by canonical RAB5 in a nucleotide state-dependent manner. Intriguingly, the subcellular localizations of EREL1 and EREL2 were also affected by coexpressed ARA7 in a nucleotide state-dependent manner (Figure 4B and 4C), although the interaction between ARA7 and EREL proteins was not detected by the yeast two-hybrid method.

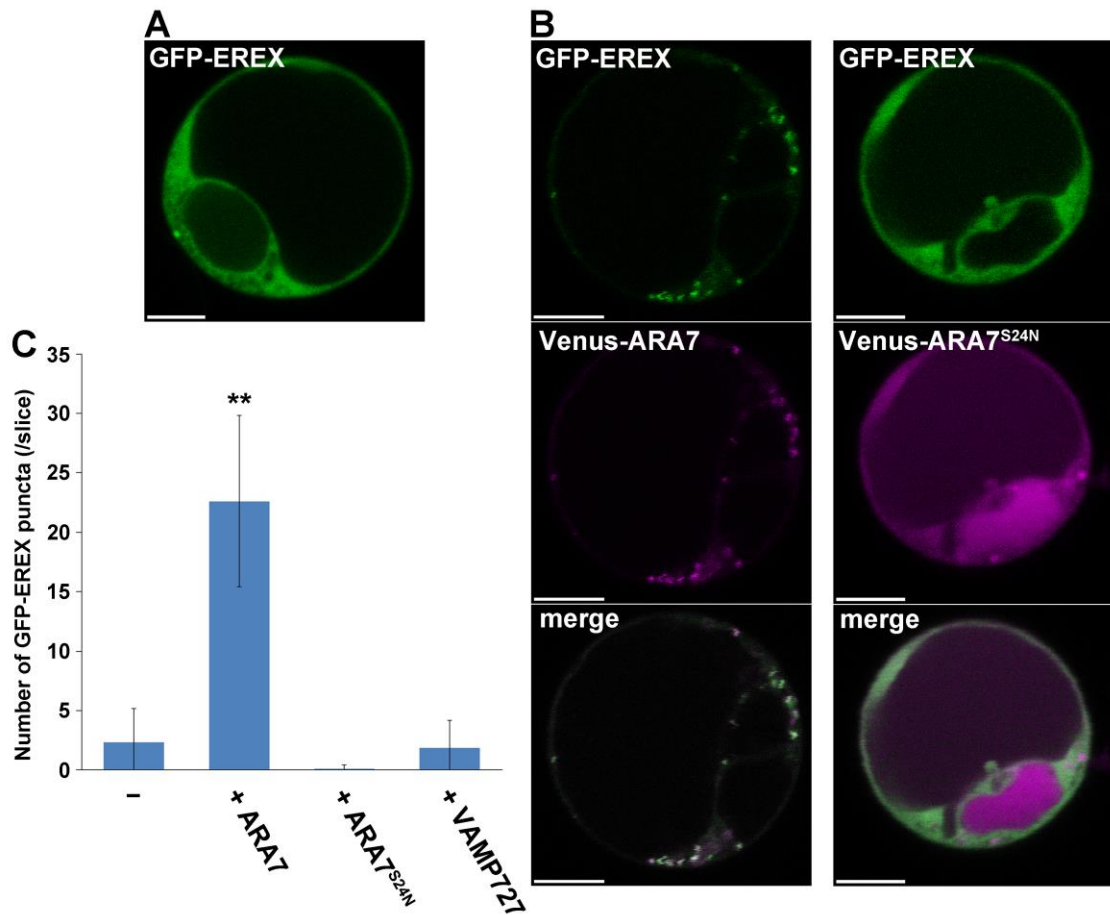


Figure 3. ARA7-dependent recruitment of EREX to the endosome

(**A**, **B**) XFP-tagged proteins were expressed transiently in the protoplasts of suspension-cultured *Arabidopsis* cells. Bars = 5 μm . (**A**) When expressed alone, GFP-EREX was mainly observed in the cytosol. (**B**) When coexpressed, wild-type ARA7 and EREX colocalized to the same endosomes (left panels), whereas coexpression of EREX with dominant negative ARA7 (ARA7^{S24N}) resulted in the dispersal of EREX into the cytosol (right panels). (**C**) Numbers of GFP-EREX-positive puncta in protoplasts expressing GFP-EREX and wild-type ARA7 or ARA7^{S24N}. The results are presented as the means \pm standard deviation ($n = 12$ confocal sections of protoplasts for GFP-EREX alone, $n = 13$ for coexpression with Venus-ARA7, $n = 18$ for coexpression with Venus-ARA7^{S24N}, and $n = 7$ for coexpression with Venus-VAMP727). ** $P < 0.01$, Tukey-Kramer test.

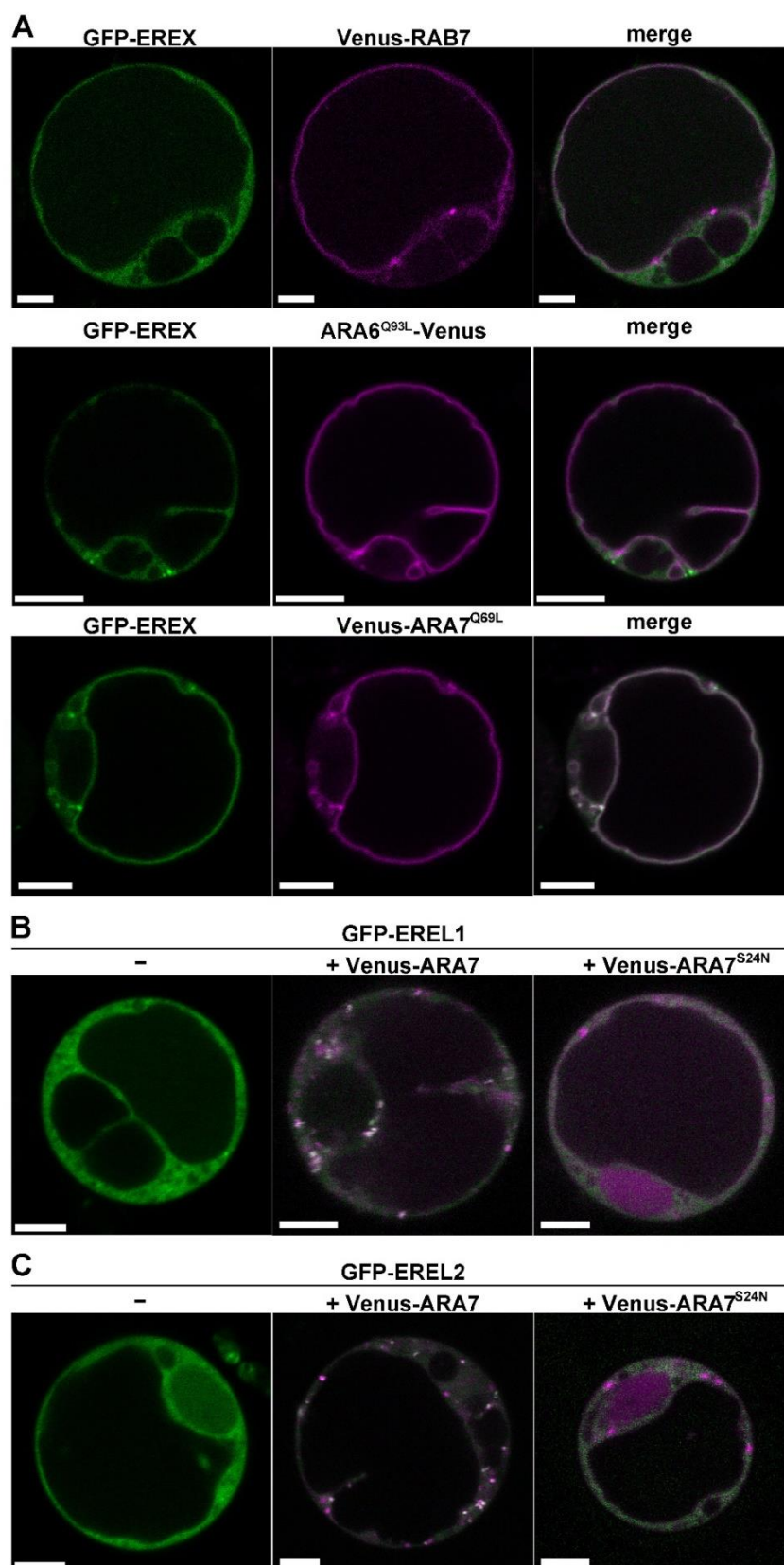


Figure 4. Colocalization of EREX and EREL with RAB5/RABF and RAB7/RABG3b

(A) GFP-tagged EREX was transiently coexpressed with Venus-tagged RAB7/RABG3b, ARA6^{Q93L} or ARA7^{Q69L}. GFP-EREX was not colocalized with Venus-tagged RAB7/RABG3b (upper panels) and ARA6^{Q93L} (middle panels), whereas Venus-ARA7^{Q69L} recruited GFP-EREX to the vacuolar membrane. **(B)** GFP-tagged EREL1 was transiently expressed in the protoplast solely (left) or coexpressed with either Venus-fused wild-type (middle) or dominant negative ARA7 (S24N; right). **(C)** GFP-tagged EREL2 was transiently expressed in the protoplast solely (left) or coexpressed with either Venus-fused wild-type (middle) or dominant negative ARA7 (S24N; right). Bars = 5 μ m.

2.4 Characterization of *erex* and *erel* mutants

To understand the functions of *EREX*, *EREL1*, and *EREL2* in *planta*, I characterized T-DNA tagged mutants of these genes (Figure 5A). I confirmed that the full-length transcript was not detected in each mutant plant (Figure 5B). Although the absence of *EREX* and *EREL* transcripts suggested that these mutants are null alleles (Figure 5B), abnormalities in plant morphology and fertility were not detected in these mutants. To determine the functional interactions between RAB5 and *EREX* and *EREL*, I examined the genetic interaction between *erex* or *erel* and *vps9a-2*, which is a weak mutant allele of the RAB5 GEF responsible for activating all RAB5 members in *Arabidopsis* (Goh et al., 2007; Sunada et al., 2016). I crossed *vps9a-2* and *erex* or *erel* mutants to generate double mutants and found that *vps9a-2 erex* and *vps9a-2 erel* double mutant plants could not be established, most likely because these double mutants were defective in gametogenesis and/or embryogenesis (Table 1 and 2). To further understand the effects of these double mutations, I conducted cross-pollination analyses using the *vps9a-2 erex* double mutant. When I crossed female mutant plants with homozygous *erex* and hemizygous *vps9a-2* mutations (*vps9a-2^{+/-}erex^{-/-}*) and male wild-type plants (Col-0), the double mutation was transferred to 34% of the progeny, suggesting that the *vps9a-2 erex* mutation had slightly reduced viability in the female gametophyte. I then crossed male *vps9a-2^{+/-}erex^{-/-}* and female Col-0 plants. The *vps9a-2 erex* mutation was transferred to only 7% of the progeny (Table 3). Thus, the double mutation affected the function or formation of the male gametophyte more severely than

it did the female gametophyte. However, the production of a double homozygous mutant is still theoretically possible at low frequency because the male and female gametophytes were not completely sterile, although we failed to establish a *vps9a-2 erex* double mutant. I examined cleared seedpods harvested from the *vps9a-2^{+/-} erex^{-/-}* mutants and found that embryos at retarded developmental stages were present at a low frequency. This result suggests that the double homozygous mutation of *vps9a-2 erex* results in embryonic lethality, which is consistent with the embryonic lethal phenotype of the *vps9a-1* mutant, a null allele of *vps9a* (Figure 6A; Goh et al., 2007).

Similarly defective embryos were also observed in cleared seedpods from the *vps9a-2^{+/-} erell^{-/-}* mutant (Figure 6A). The double homozygous *vps9a-2 erell* mutation should result in embryonic lethality without having a deleterious effect on gametophyte viability based on the progeny segregation ratio derived from the *vps9a-2^{+/-} erell^{-/-}* mutant plants (Table 2). The *vps9a-2 erel2* double mutant was indistinguishable from the *vps9a-2* mutant (Figure 5C).

The synergistic genetic interaction between *vps9a-2* and *erex* or *erell* strongly suggests that EREX and EREL1 act in the same genetic (and trafficking) pathway as VPS9a, which further supports the hypothesis that EREX acts as an effector of RAB5.

Because *erex* and *erell* exerted similar effects on the *vps9a-2* mutation, I next examined the genetic interaction between *erex* and *erell*. Consistent with the notion that EREX and EREL1 act in the same trafficking event, the *erex erell* double mutant exhibited severe growth retardation at a juvenile stage (Figure 5D and 6B). Interestingly,

this growth defect was not persistent, and the *erex erell1* double mutant eventually grew to a size similar to that of wild-type plants (Figure 5E). These phenotypes of the double mutant were restored by introducing either the genomic fragment of *EREX* containing the GFP cDNA insert or the genomic fragment of *EREL1* into the mutant background (Figure 5F), indicating that the observed phenotypes could be attributed to defective *EREX* and *EREL1*. The *erex erel2* and *erell1 erel2* double mutants were indistinguishable from wild-type plants (Figure 5D). These results indicate that *EREX* and *EREL1* play redundant functions, which are especially important in embryogenesis and/or early developmental processes after germination. Intriguingly, I could not recover the *erex erell1 erel2* triple mutant, most likely because of the partial deficiencies in the male gametophyte with the triple mutation and embryonic lethality of the triple homozygous mutant plant (Table 4 and 5 and Figure 6A). Thus, *EREL2* might partly share a common function with *EREX* and *EREL1*, although its contribution cannot be substantial given the weak genetic interaction between *vps9a-2* and *erel2*.

If *EREX* acts as an effector of canonical RAB5 and the growth defect observed in the *erex erell1* mutant is caused by defective membrane trafficking involving RAB5, it is possible that overexpression of constitutively active RAB5 could suppress the *erex erell1* phenotypes. To test this possibility, I overexpressed constitutively active ARA6 or ARA7 tagged with GFP under the control of the 35S promoter in the *erex erell1* mutant. As expected, the growth defects at the early developmental stages were partially, but significantly, suppressed by constitutively active ARA7 but not by constitutively active

ARA6 (Figure 6C). This result further supports the hypothesis that EREX acts as an effector of canonical RAB5 in RAB5-mediated trafficking events.

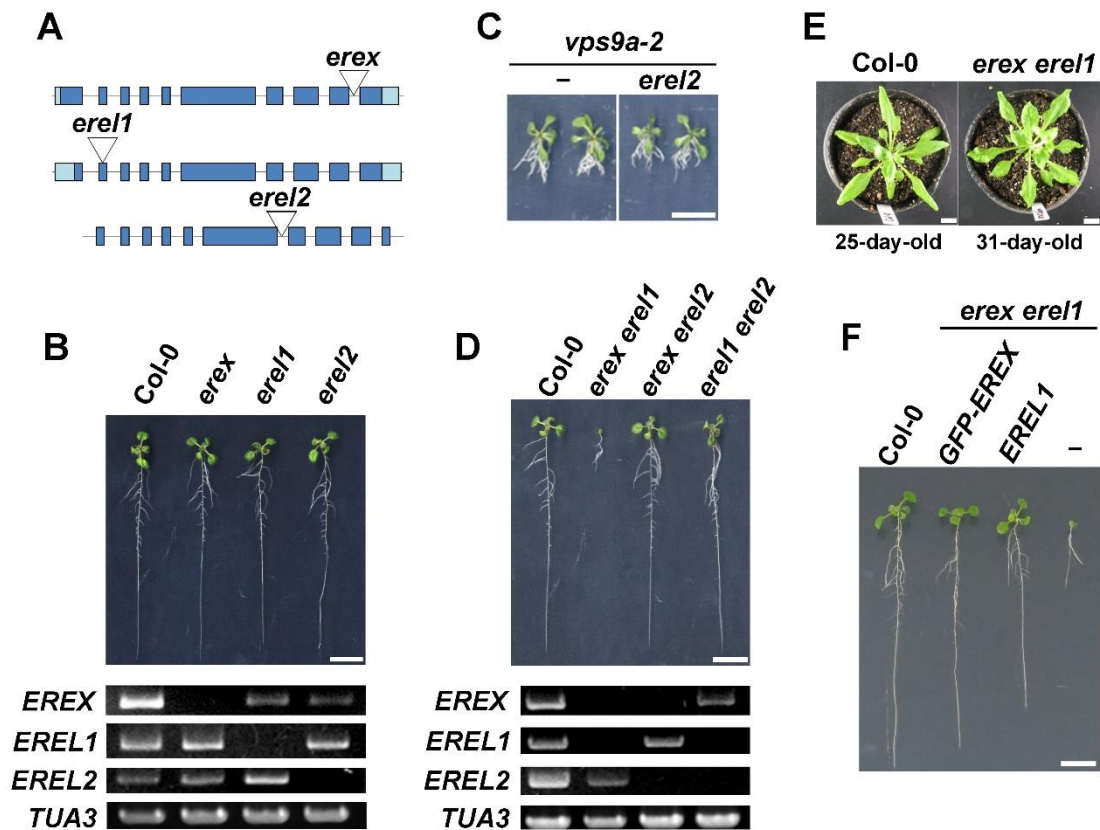


Figure 5. Characterization of *erex* and *erel* mutants

(A) Schematic structures of the *EREX* genes and the positions of T-DNA insertions. (B) Phenotypes of *erex* single mutants. Ten-day-old wild-type and mutant plants (upper panel) and expression level of *EREX* genes in plants (lower panels) with the indicated genotypes are presented. (C) The *erel2* mutation did not enhance the *vps9a-2* mutation. Twelve-day-old plants are presented. (D) Phenotypes of double mutants of *erex* and *erel* members. Ten-day-old wild-type and mutant plants (upper panel) and expression levels of *EREX* genes in the plants (lower panels) are presented. The growth of the *erex erel1* mutant was severely affected. (E) The growth phenotype in the *erex erel1* mutant was specific to the juvenile stage. Twenty-five-day-old wild-type and 31-day-old *erex erel1* mutant are presented. (F) Ten-day-old wild type and *erex erel1* double mutant seedlings expressing GFP-*EREX* or *EREL1*. The rightmost plant is the *erex erel1* double mutant. Bars = 1 cm.

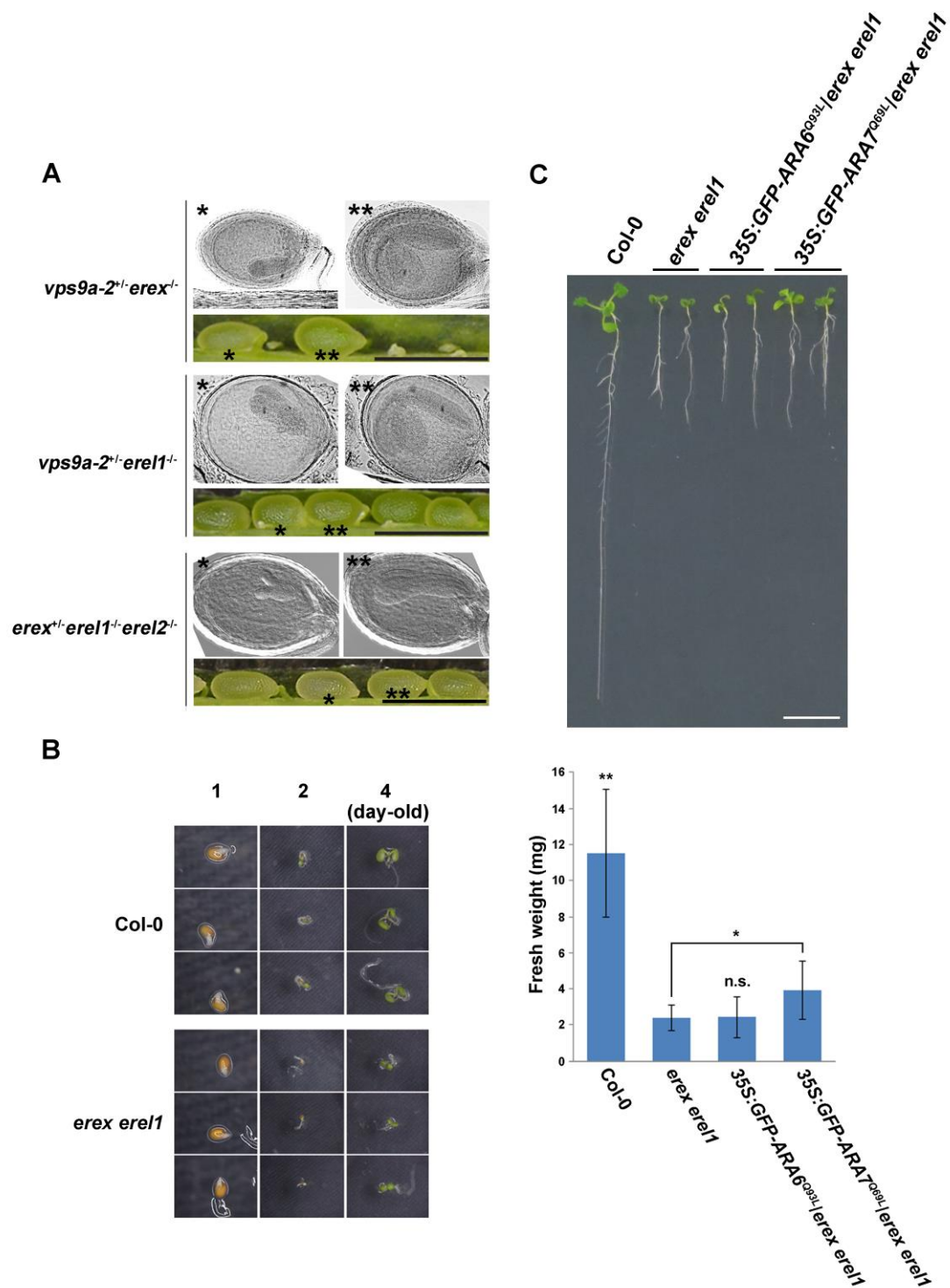


Figure 6. Characterization of the *erex* and *erel* mutants

(A) The *vps9a-2 erex* and *vps9a-2 erel1* double mutations and the *erex erel1 erel2* triple mutation caused severe retardation in embryo development. Seed pods harvested from the plants with homozygous *vps9a-2* and hemizygous *erex* or *erel1* and homozygous *erel1 erel2* and hemizygous *erex* were cleared and embryos were observed. Embryos in developing seeds marked with asterisks are presented in the upper panels. Bars = 1 mm.

(B) Time-sequential observation of wild-type (Col-0) and the *erex erell* mutant after germination. **(C)** Overexpression of constitutively active ARA7 (ARA7^{Q69L}) partially suppressed the phenotype of the *erex erell* mutant. Ten-day-old wild-type and *erex erell* plants with or without overexpressing ARA6^{Q93L} or ARA7^{Q69L} are presented (upper panel), and average fresh weights of plants with each genotype were measured (lower panel). The results are presented as the means \pm standard deviation ($n = 46$ plants for Col-0, $n = 40$ for *erex erell*, $n = 22$ for Pro35S:GFP-ARA6^{Q93L}/*erex erell*, and $n = 65$ for Pro35S:GFP-ARA7^{Q69L}/*erex erell*). * $P < 0.05$, ** $P < 0.01$, and n.s.: non-significant, Tukey-Kramer test. Bar = 1 cm.

Tables

Table 1. Segregation analysis of *vps9a-2*^{+/-} *erex*^{-/-} mutants

Genotype of progenies	<i>vps9a-2</i> ^{+/+}	<i>vps9a-2</i> ^{+/-}	<i>vps9a-2</i> ^{-/-}
	185 (61%)	120 (39%)	0 (0%)

Progenies from plants that were homozygous for *erex* and heterozygous for *vps9a-2* were genotyped by PCR.

Table 2. Segregation analysis of *vps9a-2*^{+/-} *erell*^{-/-} mutants

Genotype of progenies	<i>vps9a-2</i> ^{+/+}	<i>vps9a-2</i> ^{+/-}	<i>vps9a-2</i> ^{-/-}
	94 (34%)	182 (66%)	0 (0%)

Progenies from plants that were homozygous for *erell* and heterozygous for *vps9a-2* were genotyped by PCR.

Table 3. Cross-pollination analysis of the *vps9a-2*^{+/-} *erex*^{-/-} mutant

Male Col-0 was crossed with	Genotype of progenies	<i>vps9a-2</i> ^{+/+}	<i>vps9a-2</i> ^{+/-}
female <i>vps9a-2</i> ^{+/-} <i>erex</i> ^{-/-}		41 (66%)	21 (34%)
Male <i>vps9a-2</i> ^{+/-} <i>erex</i> ^{-/-} was	Genotype of progenies	<i>vps9a-2</i> ^{+/+}	<i>vps9a-2</i> ^{+/-}
crossed with female Col-0		51 (93%)	4 (7%)

Plants yielded by cross-pollination between Col-0 and the plant that was homozygous for *erex* and heterozygous for *vps9a-2* were genotyped by PCR.

Table 4. Segregation analysis of the *erex*^{+/-} *erel1*^{-/-} *erel2*^{-/-} mutants

Genotype of progenies	<i>erex</i> ^{+/+}	<i>erex</i> ^{+/-}	<i>erex</i> ^{-/-}	not germinated
	135 (49%)	131 (47%)	0 (0%)	11 (4%)

Progenies from plants that were homozygous for *erel1* and *erel2* and heterozygous for *erex* were genotyped by PCR.

Table 5. Cross-pollination analysis of the *erex*^{+/-} *erel1*^{-/-} *erel2*^{-/-} mutant

Male Col-0 was crossed with female <i>erex</i> ^{+/-} <i>erel1</i> ^{-/-} <i>erel2</i> ^{-/-}	Genotype of progenies	<i>erex</i> ^{+/+}	<i>erex</i> ^{+/-}
		41 (49%)	43 (51%)
Male <i>erex</i> ^{+/-} <i>erel1</i> ^{-/-} <i>erel2</i> ^{-/-} was crossed with female Col-0	Genotype of progenies	<i>erex</i> ^{+/+}	<i>erex</i> ^{+/-}
		44 (86%)	7 (14%)

Plants yielded by cross-pollination between Col-0 and the plant that was homozygous for *erel1* and *erel2* and heterozygous for *erex* were genotyped by PCR.

2.5 Expression and subcellular localization of EREX in plants

Because *EREX* performs an important function in early developmental processes as described above, I expected that *EREX* would be expressed at this stage. To examine the expression pattern of *EREX*, I constructed transgenic Arabidopsis plants expressing a translational fusion of the first exon of *EREX* and the cDNA for β -glucuronidase (GUS) under the control of the 1.6 kb *EREX* promoter. GUS staining indicated that *EREX* was abundantly expressed in young seedlings, and its expression was also observed in young leaves, root tips, and developing embryos (Figure 7). A similar expression pattern was also observed in transgenic Arabidopsis plants expressing GFP-tagged *EREX* under the control of its own regulatory elements, including the promoter, introns, and terminator (Figure 8A). GFP-*EREX* was localized to punctate compartments and to the cytosol in the cells of root tips and embryos. This construct restored the growth retardation phenotype of the *erex erell* double mutant (Figure 5F), indicating that the GFP-tagged *EREX* protein retained its original function. To analyze the identity of the *EREX*-positive compartments, I crossed this transgenic plant with plants expressing fluorescently tagged organelle markers and found that GFP-*EREX* was almost completely colocalized with mRFP-ARA7 (Figure 8B). GFP-*EREX* was not colocalized with a TGN marker, VHA-a1-mRFP, whereas GFP-*EREX* and VHA-a1-mRFP were occasionally located in close proximity to each other (Figure 8C). These results indicate that *EREX* localized to multivesicular endosomes bearing ARA7 *in planta* in a manner that was consistent with the results from transient expression in

protoplasts.

EREX harbors a PX domain, which is known to bind phosphatidylinositol 3'-monophosphate (PtdIns(3)*P*) with a few exceptions (van Leeuwen et al., 2004). To examine the requirement of phosphoinositide binding for the endosomal localization of EREX, I treated transgenic plant expressing GFP-EREX under the control of its own promoters with wortmannin, an inhibitor of phosphoinositide 3- and 4-kinases in plants (Matsuoka et al., 1995). As shown in Figure 8D, GFP-EREX was dispersed into the cytosol upon wortmannin treatment. This result suggests that EREX binds PtdIns(3)*P*, as reported for PX domain-containing proteins in other organisms, which was further supported by a lipid binding assay. I carried out a protein-lipid blot assay using membrane-immobilized phosphoinositides and a truncated version of EREX (GST-EREX⁶⁵⁻²⁷³) and detected specific binding of purified GST-EREX⁶⁵⁻²⁷³ to PtdIns(3)*P* (Figure 8E). These results indicate that PtdIns(3)*P* binding via the PX domain is required for the endosomal localization of EREX.

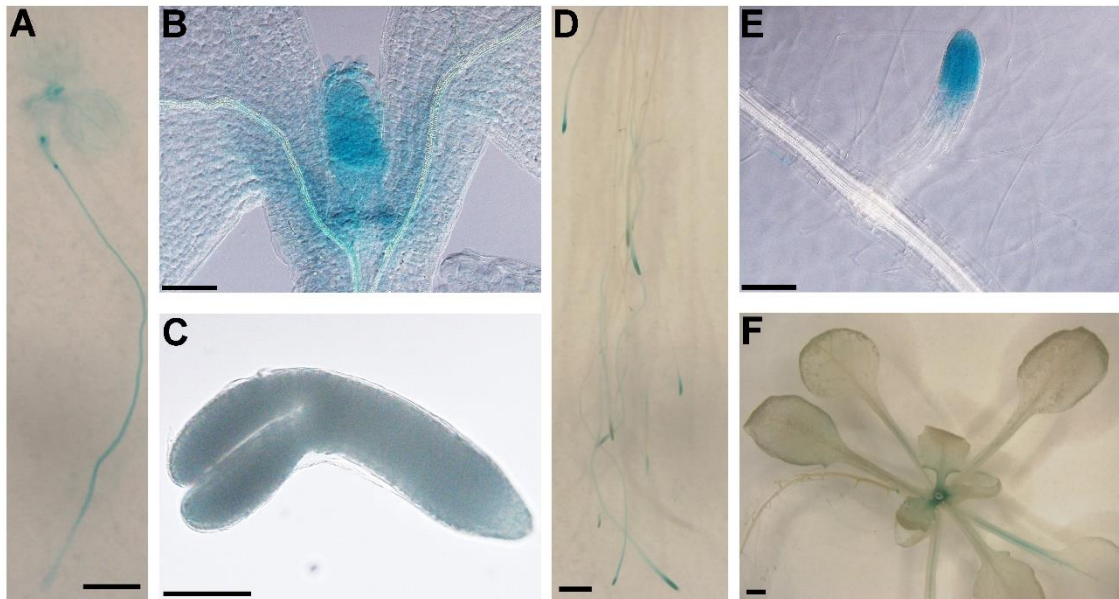


Figure 7. Promoter-reporter assay of *EREX*

(**A-F**) cDNA for GUS was connected to the first in-frame exon of *EREX* and introduced into the wild-type plant. The chimeric protein was expressed throughout the 3-day-old seedling (**A**, **B**) and the developing embryo (**C**). In the fifteen-day-old plant, GUS activity was detected only around the root tip (**D**, **E**), the vascular bundles in petioles and the shoot apical meristem (**F**). Bars = 1 mm in **A**, **D**, and **F**. Bars = 100 μ m in **B**, **C**, and **E**.

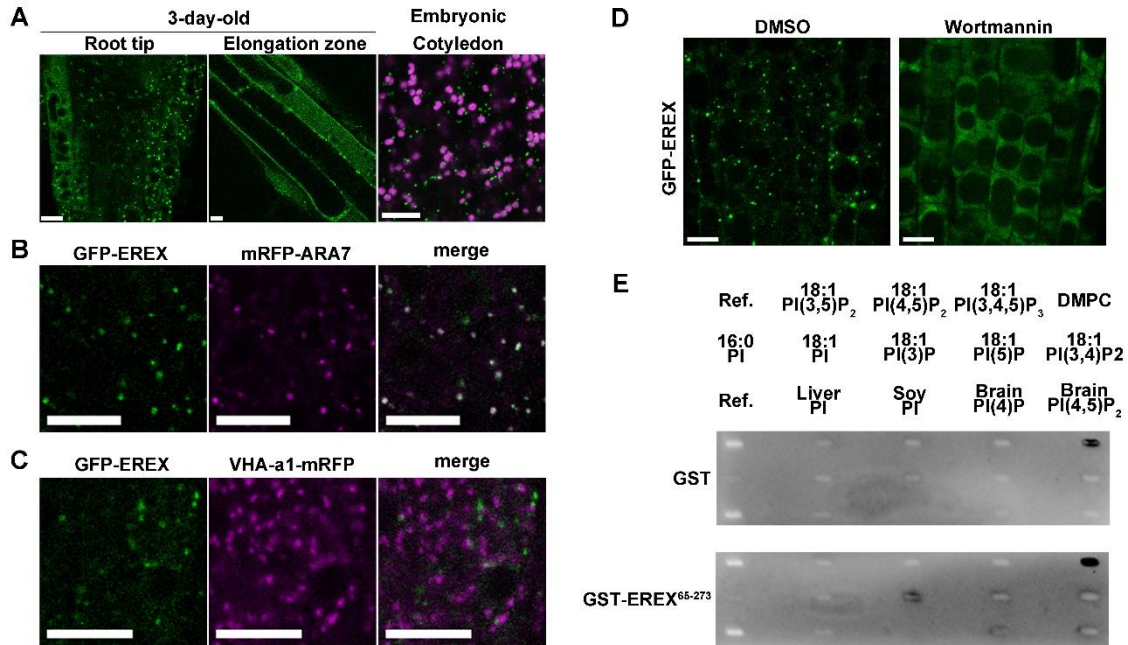


Figure 8. Localization of EREX *in planta*

(A) GFP-EREX (green) was localized to punctate compartments in epidermis cells in the root tip (left panel) and root elongation zone (middle panel) in 3-day-old *erex erell* seedlings expressing GFP-EREX. Similar localization patterns were also observed in embryonic cotyledons (right panel). Autofluorescence from plastids is shown in magenta. (B) GFP-EREX was colocalized with mRFP-ARA7 in 3-day-old root epidermis cells. (C) GFP-EREX and VHA-a1-mRFP exhibited distinct localization in the root epidermal cells of 3-day-old plants. (D) The 3-day-old GFP-EREX plants were treated with dimethylsulphoxide (DMSO) or 33 μ M wortmannin for 100 min. GFP-EREX signals were dispersed in the cytosol after wortmannin treatment. Bars in A-D = 10 μ m. (E) EREX protein lipid binding assay. The truncated version of EREX (EREX⁶⁵⁻²⁷³) comprising the PX domain and ARA7 binding activity was used for this assay. Purified GST or GST-tagged EREX⁶⁵⁻²⁷³ was incubated with the lipid-spotted membrane, and bound protein was detected with anti-GST antibody.

2.6 RAB5 acts upstream of EREX

After wortmannin treatment, although EREX was dispersed into the cytosol, ARA7 was retained on endosomes, which had dilated morphology (Figure 9A), as previously reported (Jaillais et al., 2007; Ebine et al., 2011). This result suggests that the recruitment of EREX onto endosomes is not required for the endosomal localization of RAB5. I further confirmed this by examining the localization of GFP-ARA7 in the *erex erell* double mutant; endosomal localization of GFP-ARA7 was observed in *erex erell* in both the presence and absence of wortmannin (Figure 9A). Conversely, I then examined the requirement of RAB5 activity for the endosomal localization of EREX by expressing GFP-EREX under the control of the 35S promoter in the *vps9a-2* mutant, which is partially defective in activating RAB5 members. Intriguingly, GFP-EREX was dispersed into the cytosol without localizing to endosomes (Figure 9B). I confirmed that the expression levels of GFP-EREX were comparable in the transgenic plants used in this experiment (Figure 10A). I also examined GFP-EREX localization in the loss-of-function mutant of ARA6, which is also activated by VPS9a. I did not observe alterations in the subcellular localization of GFP-EREX in the *ara6* mutant (Figure 9B), which indicates that the endosomal localization of GFP-EREX requires the activation of canonical RAB5 but not plant-specific ARA6. I also noticed that the expression of EREX in *vps9a-2* mutant plants slightly but significantly stunted the growth of the plant, while overexpression of EREX did not alter the growth of wild-type plants (Figure 10B and 10C). This result further suggests a functional interaction between EREX and

canonical RAB5.

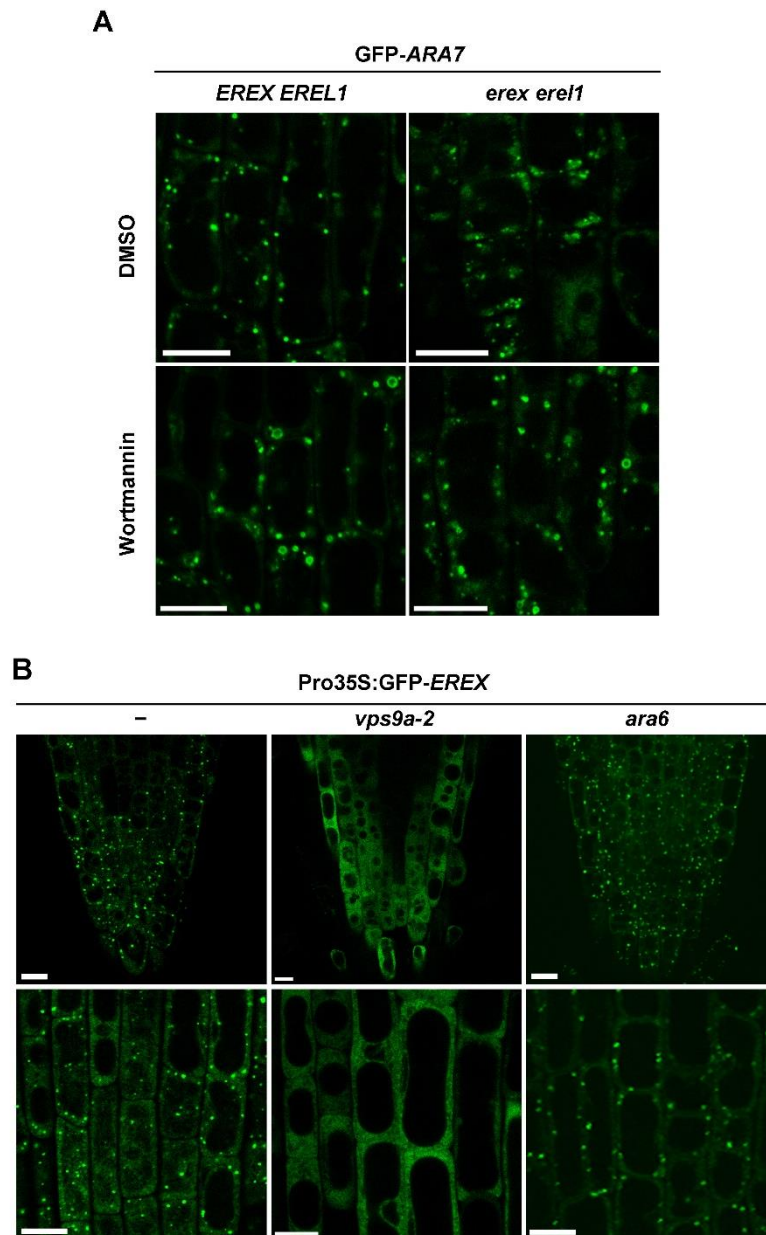


Figure 9. EREX functions downstream of canonical RAB5

(A) 4-day-old *erex erel1* and *EREX EREL1* plants were treated with DMSO or 33 μ m wortmannin for 100 min. The *ara7 rha1* mutations and the *rha1* mutation were also introduced into *EREX EREL1* and *erex erel1*, respectively, to avoid ARA7 overexpression. (B) Subcellular localization of GFP-EREX in root cells of 9-day-old wild-type, *vps9a-2* or *ara6* plants. Lower panels are magnified images of the other root epidermal cells in the same plant as those shown in the upper panels. Bars = 10 μ m.

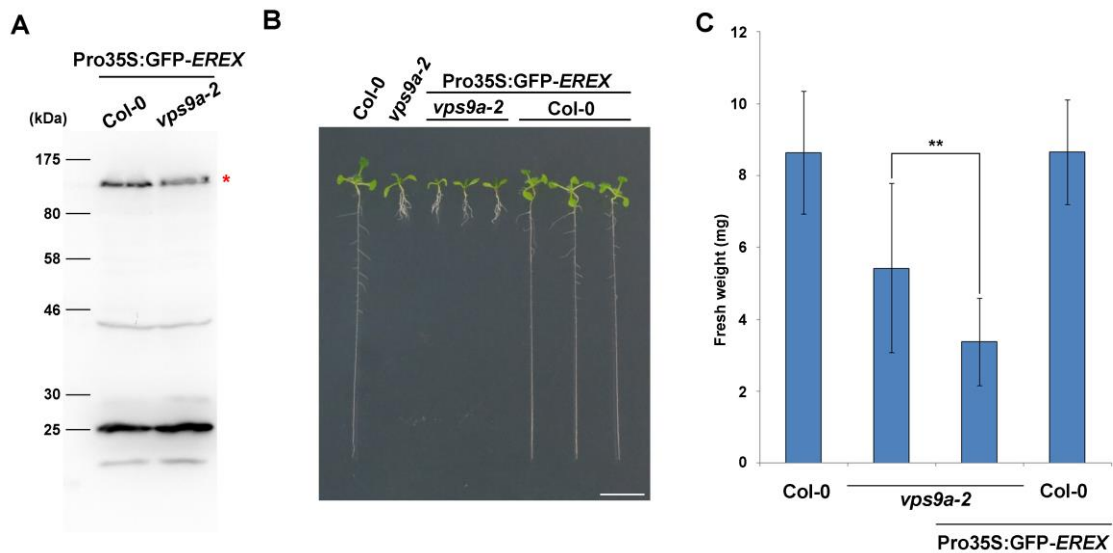


Figure 10. Overexpression of GFP-EREX in *vps9a-2*

(A) Expression levels of GFP-EREX in wild-type (Col-0) and *vps9a-2* were comparable. Samples were prepared from 9-day-old plants, and GFP-EREX (asterisk) was detected using the anti-GFP antibody. (B) Ten-day-old wild-type and *vps9a-2* plants with or without overexpressing GFP-EREX. Bars = 1 cm. (C) Fresh weights of 10-day-old plants with indicated genotypes. The results are presented as the means \pm standard deviation ($n = 53$ for Col-0, $n = 68$ for *vps9a-2*, $n = 63$ for Pro35S:GFP-EREX/*vps9a-2*, and $n = 52$ for Pro35S:GFP-EREX/Col-0. ** $P < 0.01$, Tukey-Kramer test.

2.7 EREX and EREL1 are required for the vacuolar transport of storage proteins

If EREX actually acts as an effector of RAB5, I expect that EREX would be involved in endocytic and/or biosynthetic trafficking to vacuoles. I tested this by monitoring the endocytic transport of the dye FM4-64, a marker of endocytosis, and PIN2-GFP, an auxin transporter fused to GFP, in root epidermal cells of 3-day-old wild-type and *erex erell* plants, which exhibited no discernable difference (Figure 11).

Given the high expression levels of EREX in developing embryos and young seedlings and the mutant phenotype observed at early developmental stages, it is highly likely that EREX plays crucial roles in vacuolar biogenesis and/or transport during embryogenesis and germination stages. I thus investigated the trafficking of storage proteins to protein storage vacuoles (PSVs) in embryos. The morphology of PSVs in mature *erex erell* seeds, which was visualized by their autofluorescence, was not markedly affected when compared to the PSVs of wild-type and *vps9a-2* seeds (Figure 12A). I then monitored trafficking of an artificial cargo, GFP-CT24, which consists of a signal peptide, GFP, and 24 C-terminal amino acids of the α' -subunit of β -conglycinin (Nishizawa et al., 2003) to PSVs. In wild-type embryos, GFP-CT24 was observed in PSVs (Figure 12B). Conversely, GFP-CT24 was mis-secreted to extracellular spaces in the *erex erell* and *vps9a-2* mutants (Figure 12B), indicating that the *erex erell* mutations impair the trafficking pathway to PSVs. I then investigated the native cargos for PSVs, 12S globulin and 2S albumin, which are major storage proteins in Arabidopsis seeds whose precursors are processed by vacuolar processing enzymes into

mature forms in PSVs (Shimada, 2003a). I conducted SDS-PAGE of seed proteins prepared from mature seeds collected from wild-type, *erex* and/or *erel* mutant, and *vps9a-2* mutant plants, which was followed by Coomassie brilliant blue staining or immunoblotting with anti-12S globulin or anti-2S albumin antibody. Wild-type seeds accumulated only mature forms of 12S globulin (α and β subunits) and 2S albumin (Figure 12C and 12D). In contrast, *vps9a-2* mutant seeds accumulated precursors of both 12S globulin and 2S albumin (Figure 12C and 12D). Intriguingly, *erex erel1* double-mutant seeds accumulated precursors of 12S globulin, whereas substantial accumulation of 2S albumin precursors was not detected (Figure 12C and 12D). The mis-secretion of 12S globulin to the extracellular space in *vps9a-2* and *erex erel1* mutant seeds was also confirmed by immunoelectron microscopy with the anti-12S globulin antibody (Figure 12E). Precursor accumulation was not detected in seeds of *erex* and *erel* single mutants, or *erex erel2* and *erel1 erel2* double mutants. These results indicate that EREX and EREL1 are indeed involved in the transport of 12S globulin to PSVs, which is also known to involve RAB5.

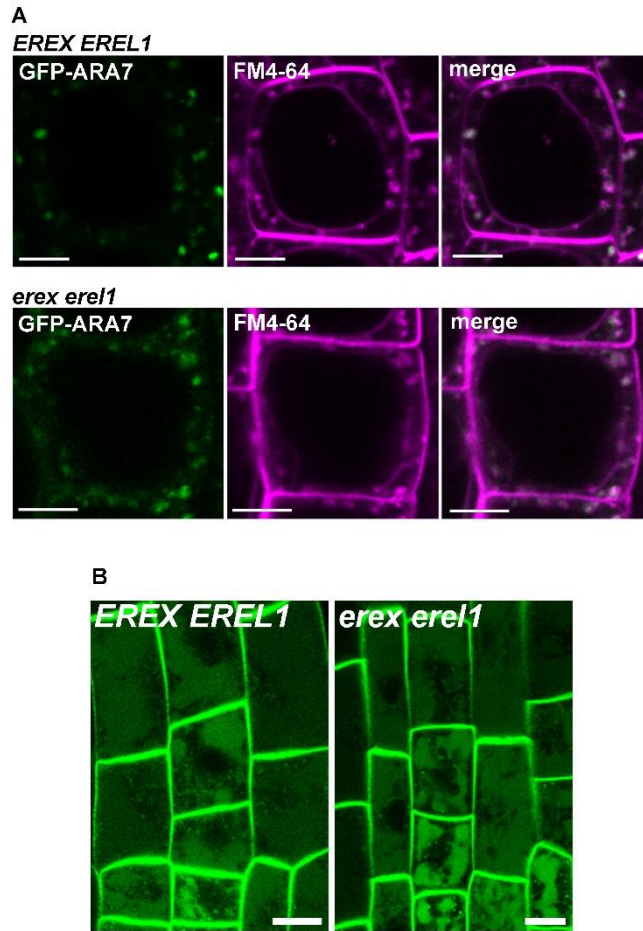


Figure 11. The *erex erel1* mutations did not affect the endocytic pathway

(A) Endocytosis of FM4-64 in the *ara7 rha1* (*EREX EREL1*) and *erex erel1 rha1* (*erex erel1*) plants expressing GFP-ARA7. Roots of 5-day-old plants were incubated in 16 μ M FM4-64 for 2 hours. (B) Endocytic transport of PIN2-GFP under dark conditions in 3-day-old wild-type (*EREX EREL1*) and *erex erel1* plants. Plants were grown under the dark condition for 2 days before observation. Bars = 10 μ m.

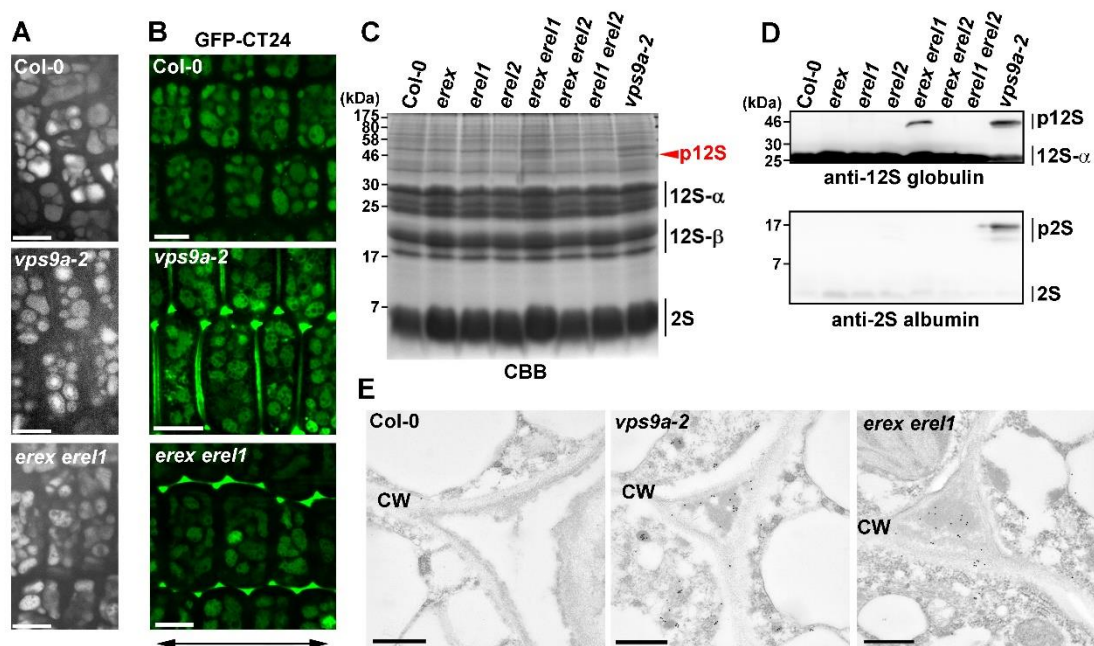


Figure 12. EREX is required for transport to the PSV

(A) The morphology of PSVs in wild-type (*Col-0*), *vps9a-2*, and *erex erel1* embryos was visualized by autofluorescence. Embryonic hypocotyl cells were observed. Bars = 10 μ m. (B) GFP-CT24 localization was observed in wild-type, *vps9a-2*, and *erex erel1* embryonic hypocotyl cells. The double-headed arrow indicates the apical-basal axis. Bars = 10 μ m. (C) Profiles of CBB-stained proteins were prepared from 40 grains of dry seeds with the indicated mutations. The arrowhead indicates precursors of 12S globulin. (D) Immunoblot analysis of proteins from dry seeds from the indicated genotypes was performed using anti-12S globulin (upper panel) and anti-2S albumin (lower panel) antibodies. p12S, precursors of 12S globulin; p2S, precursors of 2S albumin. (E) Immunoelectron micrographs of green *Col-0*, *vps9a-2*, and *erex erel1* embryos prior to desiccation with the anti-12S globulin antibody. CW, cell wall. Bars = 500 nm.

Chapter 3: Discussion

3.1 Redundant functions of EREX and EREL1 and 2

Two structurally related proteins, EREX and EREL1, exhibited distinct interaction patterns with canonical RAB5 in the yeast two-hybrid assay, in which EREX interacted with ARA7 and RHA1, whereas EREL1 was not shown to interact with these RAB5 members. However, the genetic interaction between *EREX* and *EREL1* strongly suggested that EREX and EREL1 act in the same trafficking and developmental events. The *erex erel1* double mutant exhibited deleterious phenotypes in the vacuolar transport of storage proteins and early developmental processes, whereas the single mutant of each gene was indistinguishable from the wild-type plant. Furthermore, *erex* and *vps9a-2*, as well as *erel1* and *vps9a-2*, exhibited synthetic lethality (i.e., lethality only in combination). These lines of evidence strongly suggest that EREL1 coordinates with EREX to play a pivotal role in RAB5-mediated endosomal trafficking events. Another EREX-like protein, EREL2, also appears to possess at least a partially redundant function with EREX and EREL1. Although the interaction between EREL2 and canonical RAB5 was not detected in the yeast two-hybrid assay, and the loss of function of *EREL2* did not enhance the phenotypes of the *erex*, *erel1*, and *vps9a-2* mutations, I failed to recover the *erex erel1 erel2* triple mutant. The synergistic enhancement of the growth defect of *erex erel1* by *erel2* suggested that EREL2 harbors a redundant function with EREX and EREL1, although its significance in endosomal/vacuolar trafficking remains unclear. Moreover, overexpression of constitutively active ARA7 partially

suppressed the growth defect of the *erex erell* double mutant, suggesting the possibility that abundant amount of canonical RAB5s may reinforce the function of EREL2 to compensate for the defect (Figure 13, upper left panel). The weak effect of the *erel2* mutation compared with *erell* may reflect the slightly lower expression level of *EREL2* than that of *EREL1*, which could be determined by examining public databases such as Arabidopsis eFP Browser (Winter et al., 2007).

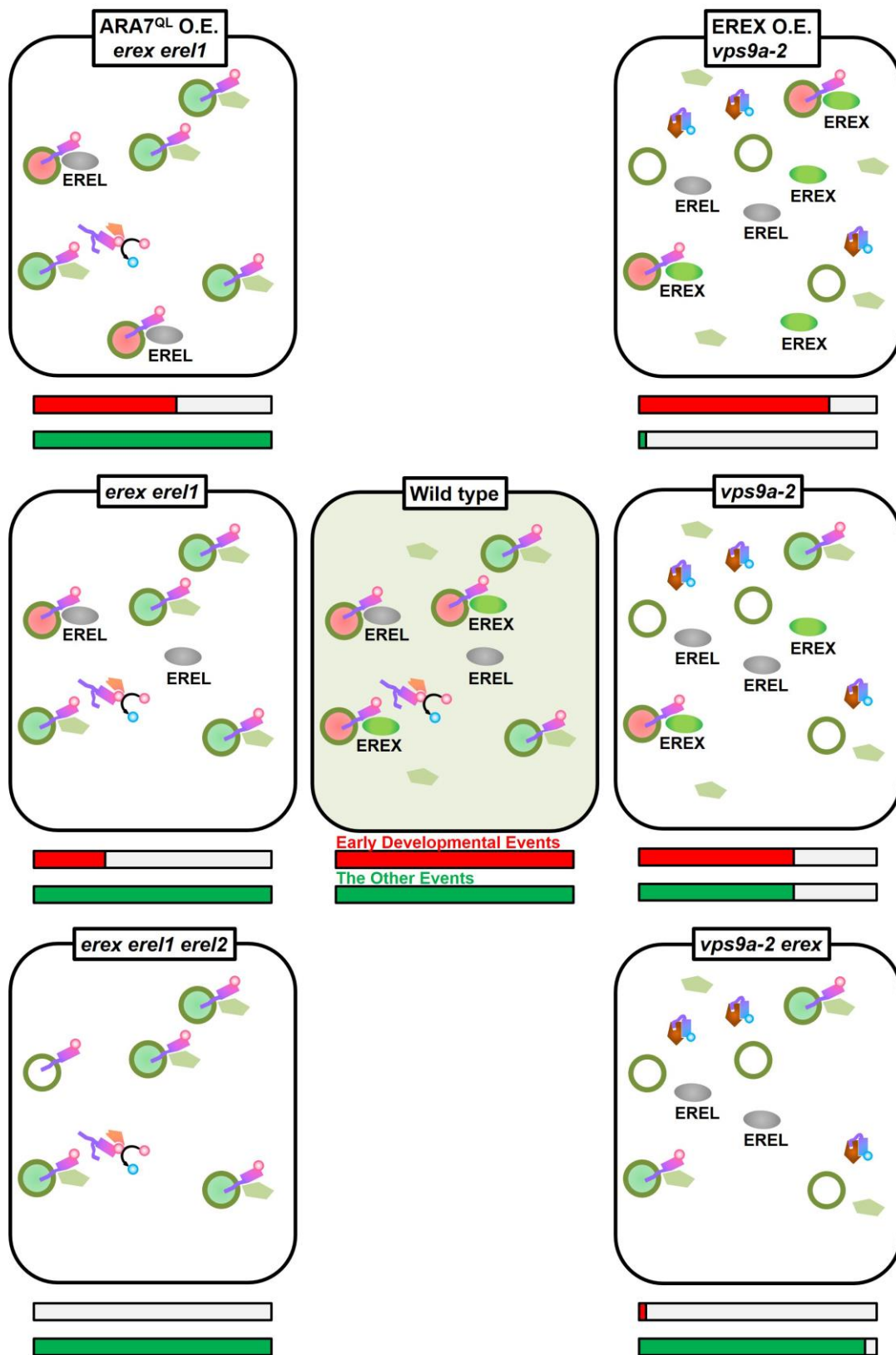


Figure 13. Schematic model of effects of the multiple mutants

3.2 Structural features of EREX/EREL members

The PX domain is a type of phosphoinositide-binding module that preferentially binds PtdIns(3)*P* (Ellson et al., 2002). Eleven PX domain-containing proteins are encoded in the Arabidopsis genome and are classified into four subgroups based on the similarity of their PX domains (van Leeuwen et al., 2004). EREX and EREL1 and 2 constitute one of these subgroups. PtdIns(3)*P* is enriched in the multivesicular endosomal membrane in plants, to which RAB5 is also localized (Gillooly et al., 2000; Vermeer et al., 2006; Simon et al., 2014). In many cases, the affinity of the PX domain for PtdIns(3)*P* is not strong enough to direct proteins to the membrane, and cooperation with other interactors is needed for PX-containing proteins to bind with membranes (Lemmon, 2008). Consistently, in the current study, the coexpression of ARA7 dramatically enhanced the endosomal localization of EREX. Meanwhile, wortmannin treatment resulted in the dissociation of EREX from the endosomal membrane. These results indicate that EREX must interact with both canonical RAB5 and the phosphoinositide to be efficiently recruited to the endosomal membrane (Figure 14). Although phosphoinositide metabolism on the endosomes has not been directly linked to RAB5 in plants, my results suggest that canonical RAB5 functions in close association with phosphoinositides, as is the case for other plant RAB GTPases and animal RAB5 (Grosshans et al., 2006; Preuss, 2006; Camacho et al., 2009; Antignani et al., 2015).

The coiled-coil region, which is known as a protein-protein interaction motif,

was predicted to be present in the C-termini of EREX and EREL members by the COILS program (Lupas et al., 1991). Because this motif is not required for the interaction between EREX and canonical RAB5, EREX may interact with some other molecules via the coiled-coil domain. Identifying and characterizing such molecules represents a promising approach for revealing the molecular mechanism of EREX-mediated trafficking to the PSV.

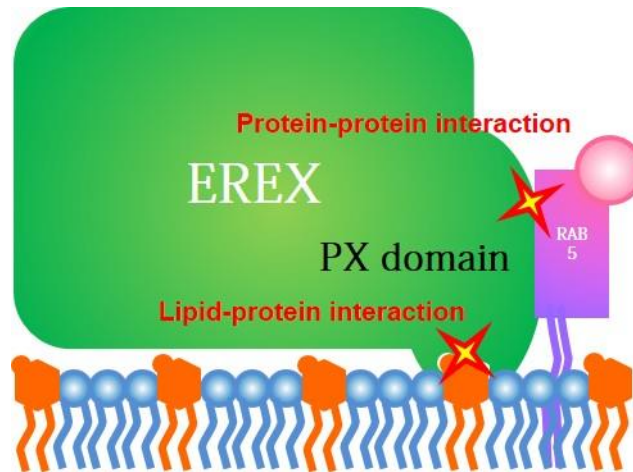


Figure 14. Schematic model of endosomal localization of EREX
Endosomal localization of EREX requires both of interactions with GTP-bound canonical RAB5 and PtdIns(3)*P*.

3.3 How does EREX mediate vacuolar trafficking with RAB5?

In this study, I focused on trafficking to PSVs because EREX was expressed abundantly in embryos and young seedlings. The phenotype of the *erex erel1* double mutant, which consists of severe growth retardation only during germination and the seedling stage, also suggests that EREX and EREL1 predominantly function during embryogenesis and/or early development of seedlings. This mutant phenotype might be accounted for by the presence of inappropriately deposited storage proteins in embryos, although it is also possible that this phenotype could be attributable to impairments in other endosomal/vacuolar functions specifically required in young seedlings. It should be noted that RAB5 members are constitutively expressed throughout development in Arabidopsis. Moreover, the *vps9a-2* mutant exhibits pleiotropic abnormalities that are not restricted to the juvenile stage. These lines of evidence suggest that distinct effector sets are recruited to the vacuolar trafficking pathways during different developmental stages. EREX and EREL members might be tailored for the RAB5-mediated trafficking pathway to PSVs, and distinct effector sets are employed in trafficking pathways to lytic vacuoles. Ectopically expressed GFP-EREX had a negative effect on the growth of *vps9a-2*. This effect might be exerted by titrating canonical RAB5 by EREX, which could result in hindered interactions between RAB5 and effectors mediating lytic vacuolar trafficking (Figure 13, upper right panel).

GFP-CT24 and 12S globulin were mis-secreted in *erex erell*, which helps confirm that EREX and EREL1 play critical roles in vacuolar trafficking in embryos in a manner consistent with the expected role of EREX as a RAB5 effector. Many mutants with similar phenotypes have been reported thus far, including mutants of vacuolar sorting receptors, vacuolar processing enzymes, and machinery components of membrane trafficking (Shimada, 2003; Shimada et al., 2003; Shimada, 2006; Tamura et al., 2007; Yamazaki et al., 2007; Ebine et al., 2008; Takahashi et al., 2010; Contento and Bassham, 2012; Shirakawa et al., 2014; Ebine et al., 2014; Gao et al., 2015; Reguera et al., 2015; Teh et al., 2015). In these mutants, the accumulation of unprocessed precursors is also observed for 2S albumin, a major storage protein in Arabidopsis seeds. *vps9a-2*, a mutant defective in the activation of RAB5, was also shown to accumulate precursors of both 12S globulin and 2S albumin. However, I did not detect accumulation of precursors of 2S albumin in the *erex erell* mutant. This phenotypic difference suggests that EREX and EREL1 are required in a specific trafficking pathway among multiple RAB5-regulated vacuolar trafficking pathways. In the experiment presented in Figure 12B, GFP-CT24 accumulation in the horizontal sides of the cells was generally observed in *vps9a-2* seeds; however, this accumulation pattern was not frequently observed in *erex erell* mutant seeds. This difference could also reflect distinct effects of the *erex erell* mutation on multiple vacuolar trafficking pathways in developing seeds, although it is also possible that these different patterns are due to the higher severity of the *vps9a-2* mutation in the transport of GFP-CT24

compared to the *erex erell* mutation. Vacuolar storage proteins have been proposed to be transported through multiple trafficking pathways to PSVs (Jolliffe et al., 2005; Vitale and Hinz, 2005). Moreover, multiple trafficking pathways involving RAB5 have been proposed to operate in vacuolar trafficking in Arabidopsis (Ebine et al., 2014). One of these trafficking pathways, which is responsible for the transport of a subpopulation of 12S globulin, might specifically involve EREX and EREL1. In some mutants defective in transport between the ER and Golgi, 12S globulin and 2S albumin are reported to accumulate in different regions of the Maigo body, an abnormal compartment derived from the ER (Li et al., 2006; Takahashi et al., 2010). Although it is not clear whether the precursors of these storage proteins are segregated in the ER in wild-type plants, some populations of 12S globulin might be transported from the ER to the vacuole via a distinct pathway from 2S albumin in an EREX- and EREL1-dependent manner. Alternatively, canonical RAB5 may regulate sorting for PSVs on the TGN, which is similar to reports in rice (*Oryza sativa*) endosperm (Ren et al., 2014; Wen et al., 2015). A subpopulation of canonical RAB5 has been localized to the TGN, which is likely responsible for maturation from the TGN to the multivesicular endosomes (Stierhof and El Kasmi, 2010; Scheuring et al., 2011; Singh et al., 2014). EREX might coordinate cargo sorting and RAB5 activity during this event, which is consistent with the findings that the mutations in AP-4 and sorting nexins that are involved in vacuolar protein transport at the TGN and RAB5-positive endosomes, respectively, exert similar effects on transport of 12S globulin and 2S albumin to the *erex erell* mutation (Fuji et

al., 2016; Pourcher et al., 2010).

3.4 Concluding Remarks

In this thesis, I demonstrated that EREX, the plant-specific PX domain-containing protein, regulates specific aspects of vacuolar transport as an effector of canonical RAB5. This may also be true for EREL members. EREX mediates vacuolar transport of distinctive proteins to PSVs, which is indispensable for the proper development of Arabidopsis at the early seedlings. Importantly, my findings indicate that a specific set of RAB5 effectors is responsible for a developmental stage-specific or cargo-specific endosomal/vacuolar trafficking pathway. In addition, the dual requirement of interactions with both ARA7 and PtdIns(3)*P* for endosomal localization of EREX may reflect a part of the mechanism to adopt a specific set of effectors with a spatial control. These spatiotemporal regulations suggest that plant RAB5 exerts its wide range of functions throughout the plant's life cycle via interactions with various effector proteins specialized for trafficking pathways and/or vacuolar functions. Further experiments aimed at isolating other effector proteins and functional analyses of these molecules are needed to unravel the complete function of RAB5 GTPases in plants.

Experimental Procedures

Yeast Two-Hybrid Assay

cDNA fragments for wild-type and mutant versions of RAB proteins without isoprenylation sites were subcloned into the EcoRI or Sall site of the pBD-GAL4 Cam vector (Stratagene). Interacting partners of constitutively active ARA7 were screened using the yeast two-hybrid method from the cDNA library prepared from the roots of 4-day-old *Arabidopsis thaliana* plants and subcloned between EcoRI and XhoI sites of the pAD-GAL4-2.1 plasmid (provided by T. Demura, NAIST). Yeast AH109 cells (Clontech; *trp1 leu2 his3 LYS2::GALI_{UAS}-GALI_{TATA}-HIS3*) expressing constitutively active ARA7 (ARA7^{Q69L}) fused to the Gal4 binding domain were transformed with the library, and positive clones were selected. After confirming reproducibility at least three times, false positives were eliminated by cotransformation with the empty vector for each candidate. Full-length cDNA fragments of *EREX* and *EREL* members were amplified by RT-PCR using total RNA prepared from Arabidopsis roots as a template, which were subcloned into the BamHI site of pAD-GAL4-2.1 vector (Stratagene) and used for subsequent experiments.

Purification of bacterially expressed proteins

The GST-fused EREX⁶⁵⁻²⁷³ protein and GST were expressed in the *Escherichia coli* Rosetta (DE3) strain (MERCK) using the pGEX4T-1 vector (GE Healthcare). Cells expressing these proteins were suspended in lysis buffer (1x PBS pH 7.4, 1% Triton

X-100, 1 mg/ml Lysozyme (Wako), 0.5 U/mL DNase I (Invitrogen), and a protease inhibitor cocktail (GE Healthcare)), sonicated, and centrifuged at $10,000 \times g$ for 40 min. Supernatants were loaded onto Glutathione-Sepharose 4B columns (GE Healthcare) and washed with 3 column volumes of washing buffer (1x PBS pH 7.4, and 1% Triton X-100), and the proteins were then eluted with elution buffer (20 mM reduced glutathione, 1x PBS pH 7.4, and 1% Triton X-100). Purification of His₆-tagged ARA6 and ARA7 was conducted as described previously (Ebine et al., 2014).

***In vitro* pull-down assay**

Purified GST-EREX⁶⁵⁻²⁷³ and RAB5-His₆ were co-incubated for 2 hr at 4°C with Glutathione-Sepharose 4B resin (GE Healthcare) in binding buffer (1x PBS pH 7.4 and 0.03% Tween-20 containing either 10 μM GTPγS (Figure 2A) or 25 μM GTPγS or GDP) (Figure 2B). Protein complexes bound to resins were washed three times with the same buffer, boiled in sample buffer with bromophenol blue and mercaptoethanol for 5 min at 95°C, and subjected to immunoblot analysis.

Antibodies

The anti-GST polyclonal antibody (Z-5; Santa Cruz Biotechnology), anti-His₆ monoclonal antibody (04905318001; Roche), and anti-GFP monoclonal antibody (GF200; Nacalai Tesque) were commercially available. Anti-2S albumin and anti-12S globulin antibodies were supplied by I. Hara-Nishimura (Kyoto University).

Plant Materials and Plasmids

erex (SALK_008160), *erell1* (SALK_114362), and *erell2* (SALK_139378) mutants were obtained from the ABRC (Alonso et al., 2003) and backcrossed at least three times with wild-type *Arabidopsis thaliana* ecotype Columbia (Col-0) was used as the wild type in this study. Transgenic plants expressing GFP-CT24, VHA-a1-mRFP, and PIN2-GFP were kindly provided by N. Maruyama (Kyoto University), K. Schumacher (Ruprecht Karls University), and J. Friml (IST Austria), respectively. Transgenic plants expressing GFP-ARA7 or mRFP-ARA7 and the *vps9a-2* mutant were retrieved from the lab stock (Goh et al., 2007; Ebine et al., 2014). For *erex* complementation, the cDNA for GFP was inserted after the start codon of the genomic fragment of *EREX*, which contained 1581 bp upstream and 701 bp downstream sequences of the coding region. This sequence was subcloned into the binary vector pGWB1 provided by T. Nakagawa (Shimane University) (Nakagawa et al., 2007), and the resulting plasmid was used to transform the *erex erell1* double mutant. For *EREL1*, the genomic fragment containing 1401 bp upstream and 879 bp downstream sequences of the coding region of *EREL1* was subcloned into pGWB1 and used for transformation. Primer sequences used for amplification of genomic fragments are listed in Supplemental Table 6. The translational fusion between GFP and *EREX* was generated by fluorescently tagging full-length proteins (Tian, 2004). For the GUS-fusion expression analysis, the genomic fragment containing the promoter region used in the complementation experiment and the first exon of *EREX* were subcloned in-frame into pGWB3 (from T. Nakagawa, Nakagawa et

al., 2007) and used to transform wild-type *Arabidopsis*. I cloned *EREX* cDNA into pGWB6 (from T. Nakagawa) (Nakagawa et al., 2007) containing the 35S promoter for overexpression of *EREX*. Transformation of *Arabidopsis* plants was performed via floral dipping using *Agrobacterium tumefaciens* (strain GV3101::pMP90) (Clough and Bent, 1998). *Arabidopsis* seeds were surface sterilized and sown onto Murashige-Skoog plates supplemented with Gamborg's vitamins (Sigma), 30 mM sucrose, and 0.7% gellan gum (Wako). After a 3-day incubation period at 4°C to break seed dormancy, *Arabidopsis* plants were grown at 23°C under continuous white light with a fluorescent lamp (FL40SW, Toshiba) and transferred to soil after 2-3 weeks.

GUS staining

Developed embryos, 3-day-old seedlings, and 15-day-old seedlings were soaked in staining solution (100 mM sodium phosphate buffer pH 7.2, 10 mM EDTA, 0.1% Triton X-100, and 0.5 mg/ml X-glucuronide) and decompressed for 15 min, followed by incubation at 37°C for 15 hr. Samples were incubated in 70% ethanol at 37°C for 2 hr, transferred to fresh 70% ethanol and incubated for 1 – 2 weeks at 4°C, and then mounted in a clearing solution (8 g of chloral hydrate in 1 ml of glycerol and 2 ml of water) on glass microscope slides.

RT-PCR

Total RNA was extracted using the RNAqueous-4PCR kit (Ambion) and treated with

DNase I (Invitrogen) to reduce genomic DNA contamination. cDNA was synthesized by SuperScript III reverse transcriptase (Invitrogen) with an oligo (dT) 18 primer. The primer sets used for PCR are listed as follows; 5'-ATGAATCTATACGCGCACGATC-3' and 5'-TCATTTCTCAAGGATCTTGCTC-3' (EREX), 5'-GCGGATCCATGATGCAGAGACGGAGTCC-3' and 5'-GCGGATCCCTATCTCTTCAATGTTTCTC-3' (EREL1), and 5'-ATGCAAAGACGGAGTCCACC-3' and 5'-TCAGTCCTCATACATATCTGCC-3' (EREL2). The PCR conditions were as follows: 95°C (2 min); 35 cycles of 95°C (30 sec), 55°C (30 sec), 72°C (90 sec), and 72°C (10 min).

Light Microscopy

Transient expression in protoplasts was conducted as described previously (Ueda et al., 2001). For single-color imaging in root cells, GFP was excited using a diode-pumped solid-state laser (Cobolt Blues, Cobolt) at 473 nm and observed under a microscope (BX51, Olympus) equipped with a confocal scanner unit (CSU10, Yokogawa Electric) and a cooled CCD (charge-coupled device) camera (ORCA-AG, Hamamatsu Photonics). Multi-color observation was carried out using an LSM510, LSM710, or LSM780 confocal microscope (Carl Zeiss). The morphology of PSVs was observed as described previously (Ebine et al., 2008). Imaging of GUS-stained plants was conducted using a stereomicroscope (MZ16FA, Leica) and a light microscope (BX60, Olympus) equipped with a CCD camera (VB-7010, Keyence, and DP73, Olympus, respectively). Samples were treated with 33 μ M wortmannin (Sigma) for phosphoinositide kinase inhibition

experiments and 16 μ M FM4-64 (Sigma) for tracing endocytosis. mRFP-ARA7, VHA-a1-mRFP, GFP-ARA7, and PIN2-GFP were observed in the root epidermal cells of 3- to 5-day-old plants. For observation of embryos, seedpods were cleared according to previously published methods (Aida et al., 1997). *vps9a-2 erex*, *vps9a-2 erell*, and *erex erell erel2* embryos were observed with either a microscope (BX52, Olympus) equipped with a confocal scanner (CSU10, Yokogawa Electric) and camera (ORCA-ER, Hamamatsu Photonics) or a microscope (DM4500B, Leica) equipped with a camera alone (DFC300FX, Leica).

Lipid-binding assay

Thirteen lipid species spotted onto a membrane (Inositol Snoopers, Avanti) were incubated for 1 hr at room temperature in wash buffer (20 mM Tris-HCl, pH 7.5, and 0.8% NaCl) containing 3% fatty acid-free BSA (Nacalai). Purified GST or GST-EREX⁶⁵⁻²⁷³ was then added at a concentration of 1 μ g/ml and incubated for 1 hr at room temperature in wash buffer supplemented with 1% fatty acid-free BSA. The membrane was washed three times for 10 min each in wash buffer, and bound GST and GST-EREX⁶⁵⁻²⁷³ were detected with anti-GST antibody (diluted 1000-fold).

Detection of seed storage proteins

SDS-PAGE and immunoblot analyses were performed as described previously (Shimada, 2003a, b). Blots were probed with anti-12S globulin α -subunit (anti-12S,

diluted 1000-fold) and anti-2S albumin (anti-2S, diluted 1000-fold) antibodies. Signals were detected using the ECL detection system (GE Healthcare). Immunoelectron microscopy was performed as described previously (Ebine et al., 2014).

Accession Numbers

The Arabidopsis Genome Initiative locus identifiers for the genes mentioned in this article are At3g15920 (EREX), At4g32160 (EREL1), At2g25350 (EREL2), At4g19640 (ARA7/RABF2b), At5g45130 (RHA1/RABF2a), At3g54840 (ARA6/RABF1), At3g19770 (VPS9a), At1g22740 (RAB75/RABG3b), At4g18430 (RABA1e), At5g57090 (PIN2), At3g54300 (VAMP727), and At2g28520 (VHA-a1).

Acknowledgments

First of all, I would like to express my appreciation to associate professor Takashi Ueda and professor Akihiko Nakano, University of Tokyo, for their supervision throughout this study.

I thank the Salk Institute for providing the Arabidopsis T-DNA insertion mutants. I also thank T. Demura (RIKEN) for cDNA expression libraries, T. Nakagawa (Shimane University) for pGWB vectors, N. Maruyama (Kyoto University) for seeds of GFP-CT24, K. Schumacher (Ruprecht Karls University) for seeds of VHA-a1-mRFP, I. Hara-Nishimura (Kyoto University) for anti-bodies against 12S globulin and 2S albumin, H. Tsukaya (University of Tokyo) for support in microscopic observation, and E. Furuyama (University of Tokyo) for backcrossing and generating multiple mutants of *erex* and *erel* members.

I appreciate all the Lab Members, especially T. Uemura, E. Ito, K. Ebine, T. Tsustui, M. Fujimoto, T. Goh, M. Sunada, T. Inoue and T. Kanazawa for insightful comments and technical supports.

Lastly, I wish to express a special thanks to my family and friends (especially A. Vigours for improving my English) for supports and encouragements throughout the years.

References

- Aida, M., Ishida, T., Fukaki, H., Fujisawa, H., and Tasaka, M.** (1997). Genes involved in organ separation in Arabidopsis: an analysis of the cup-shaped cotyledon mutant. *Plant Cell* **9**, 841-857.
- Alonso, J.M., et al.** (2003). Genome-wide insertional mutagenesis of *Arabidopsis thaliana*. *Science* **301**, 653–657.
- Antignani, V., Klocko, A.L., Bak, G., Chandrasekaran, S.D., Dunivin, T., and Nielsen, E.** (2015). Recruitment of PLANT U-BOX13 and the PI4K $\beta 1/\beta 2$ phosphatidylinositol-4 kinases by the small GTPase RabA4B plays important roles during salicylic acid-mediated plant defense signaling in Arabidopsis. *Plant Cell* **27**, 243-261.
- Asaoka, R., Uemura, T., Ito, J., Fujimoto, M., Ito, E., Ueda, T., and Nakano, A.** (2012). Arabidopsis RABA1 GTPases are involved in transport between the *trans*-Golgi network and the plasma membrane, and are required for salinity stress tolerance. *Plant J.* **73**, 240-249.
- Beck, M., Zhou, J., Faulkner, C., MacLean, D., and Robatzek, S.** (2012). Spatio-temporal cellular dynamics of the Arabidopsis Flagellin receptor reveal activation status-dependent endosomal sorting. *Plant Cell* **24**, 4205-4219.
- Benmerah, A.** (2004). Endocytosis: signaling from endocytic membranes to the nucleus. *Curr. Biol.* **14**, R314-316.
- Berson, T., von Wangenheim, D., Takáč, T., Šamajová, O., Rosero, A., Ovečka, M., Komis, G., Stelzer, E.H., and Šamaj, J.** (2014). *trans*-Golgi network localized small GTPase RabA1d is involved in cell plate formation and oscillatory root hair growth. *BMC Plant Biol.* **14**, 252-252.
- Bottanelli, F., Gershlick, D.C., and Denecke, J.** (2012). Evidence for sequential action of Rab5 and Rab7 GTPases in prevacuolar organelle partitioning. *Traffic* **13**, 338-354.
- Bottanelli, F., Foresti, O., Hanton, S., and Denecke, J.** (2011). Vacuolar transport in

tobacco leaf epidermis cells involves a single route for soluble cargo and multiple routes for membrane cargo. *Plant Cell* **23**, 3007-3025.

Camacho, L., Smertenko, A.P., Perez-Gomez, J., Hussey, P.J., and Moore, I. (2009). Arabidopsis Rab-E GTPases exhibit a novel interaction with a plasma-membrane phosphatidylinositol-4-phosphate 5-kinase. *J. Cell Sci.* **122**, 4383-4392.

Choi, S.w., Tamaki, T., Ebine, K., Uemura, T., Ueda, T., and Nakano, A. (2013). RABA members act in distinct steps of subcellular trafficking of the FLAGELLIN SENSING2 receptor. *Plant Cell* **25**, 1174-1187.

Chow, C.M., Neto, H., Foucart, C., and Moore, I. (2008). Rab-A2 and Rab-A3 GTPases define a *trans*-golgi endosomal membrane domain in Arabidopsis that contributes substantially to the cell plate. *Plant Cell* **20**, 101-123.

Christoforidis, S., and Zerial, M. (2000). Purification and identification of novel Rab effectors using affinity chromatography. *Methods* **20**, 403-410.

Christoforidis, S., Miaczynska, M., Ashman, K., Wilm, M., Zhao, L., Yip, S.C., Waterfield, M.D., Backer, J.M., and Zerial, M. (1999). Phosphatidylinositol-3-OH kinases are Rab5 effectors. *Nat. Cell Biol.* **1**, 249-252.

Clough, S.J., and Bent, A.F. (1998). Floral dip: a simplified method for *Agrobacterium*-mediated transformation of *Arabidopsis thaliana*. *Plant J.* **16**, 735-743.

Contento, A.L., and Bassham, D.C. (2012). Structure and function of endosomes in plant cells. *J. Cell Sci.* **125**, 3511-3518.

Cui, Y., Zhao, Q., Gao, C., Ding, Y., Zeng, Y., Ueda, T., Nakano, A., and Jiang, L. (2014). Activation of the Rab7 GTPase by the MON1-CCZ1 complex is essential for PVC-to-Vacuole trafficking and plant growth in Arabidopsis. *Plant Cell.* **26**, 2080-2097.

de Graaf, P., Zwart, W.T., van Dijken, R.A., Deneka, M., Schulz, T.K., Geijsen, N.,

- Coffer, P.J., Gadella, B.M., Verkleij, A.J., van der Sluijs, P., and van Bergen en Henegouwen P.M.** (2004). Phosphatidylinositol 4-kinase beta is critical for functional association of rab11 with the Golgi complex. *Mol. Biol. Cell* **15**, 2038-2047.
- Dettmer, J.** (2006). Vacuolar H⁺-ATPase activity is required for endocytic and secretory trafficking in Arabidopsis. *Plant Cell* **18**, 715-730.
- Dhonukshe, P., Baluška, F., Schlicht, M., Hlavacka, A., Šamaj, J., Friml, J., and Gadella Jr, T.W.J.** (2006). Endocytosis of cell surface material mediates cell plate formation during plant cytokinesis. *Dev. Cell* **10**, 137-150.
- Dhonukshe, P.** (2009). Cell polarity in plants: Linking PIN polarity generation mechanisms to morphogenic auxin gradients. *Commun. Integr. Biol.* **2**, 184–190.
- D'Souza-Schorey, C., and Chavrier, P.** (2006). ARF proteins: roles in membrane traffic and beyond. *Nat. Rev. Mol. Cell Biol.* **7**, 347-358.
- Ebine, K., and Ueda, T.** (2008). Unique mechanism of plant endocytic/vacuolar transport pathways. *J. Plant Res.* **122**, 21-30.
- Ebine, K., Inoue, T., Ito, J., Ito, E., Uemura, T., Goh, T., Abe, H., Sato, K., Nakano, A., and Ueda, T.** (2014). Plant vacuolar trafficking occurs through distinctly regulated pathways. *Curr. Biol.* **24**, 1375-1382.
- Ebine, K., Okatani, Y., Uemura, T., Goh, T., Shoda, K., Niihama, M., Morita, M.T., Spitzer, C., Otegui, M.S., Nakano, A., and Ueda, T.** (2008). A SNARE complex unique to seed plants is required for protein storage vacuole biogenesis and seed development of *Arabidopsis thaliana*. *Plant Cell* **20**, 3006-3021.
- Ebine, K., Fujimoto, M., Okatani, Y., Nishiyama, T., Goh, T., Ito, E., Dainobu, T., Nishitani, A., Uemura, T., Sato, M.H., Thordal-Christensen, H., Tsutsumi, N., Nakano, A., and Ueda, T.** (2011). A membrane trafficking pathway regulated by the plant-specific RAB GTPase ARA6. *Nat. Cell Biol.* **13**, 853-859.
- Ellson, C.D., Andrews, S., Stephens, L.R., and Hawkins, P.T.** (2002). The PX domain: a new phosphoinositide-binding module. *J. Cell Sci.* **115**, 1099-1105.

- Epp, N., Rethmeier, R., Krämer, L., and Ungermann, C.** (2011). Membrane dynamics and fusion at late endosomes and vacuoles-Rab regulation, multisubunit tethering complexes and SNAREs. *Eur. J. Cell Biol.* **90**, 779-785.
- Feraru, E., Feraru, M.I., Asaoka, R., Paciorek, T., De Rycke, R., Tanaka, H., Nakano, A., and Friml, J.** (2012). BEX5/RabA1b regulates *trans*-Golgi network-to-plasma membrane protein trafficking in Arabidopsis. *Plant Cell* **24**, 3074-3086.
- Friml, J.** (2010). Subcellular trafficking of PIN auxin efflux carriers in auxin transport. *Eur. J. Cell Biol.* **89**, 231-235.
- Fuji, K., Shirakawa, M., Shiono, Y., Kunieda, T., Fukao, Y., Koumoto, Y., Takahashi, H., Hara-Nishimura, I., and Shimada, T.** (2016). The adaptor complex AP-4 regulates vacuolar protein sorting at the *trans*-Golgi network by interacting with VACUOLAR SORTING RECEPTOR1. *Plant Physiol.* **170**, 211-219.
- Galvez, T., Gilleron, J., Zerial, M., and O'Sullivan, G.A.** (2012). SnapShot: Mammalian Rab proteins in endocytic trafficking. *Cell* **151**, 234-234.e232.
- Gao, C., Zhuang, X., Cui, Y., Fu, X., He, Y., Zhao, Q., Zeng, Y., Shen, J., Luo, M., and Jiang, L.** (2015). Dual roles of an Arabidopsis ESCRT component FREE1 in regulating vacuolar protein transport and autophagic degradation. *Proc. Natl. Acad. of Sci. USA* **112**, 1886-1891.
- Gillooly, D.J., Morrow, I.C., Lindsay, M., Gould, R., Bryant, N.J., Gaullier, J.M., Parton, R.G., and Stenmark, H.** (2000). Localization of phosphatidylinositol 3-phosphate in yeast and mammalian cells. *EMBO J.* **19**, 4577-4588.
- Goh, T., Uchida, W., Arakawa, S., Ito, E., Dainobu, T., Ebine, K., Takeuchi, M., Sato, K., Ueda, T., and Nakano, A.** (2007). VPS9a, the common activator for two distinct types of Rab5 GTPases, is essential for the development of *Arabidopsis thaliana*. *Plant Cell* **19**, 3504-3515.
- Goody, R.S., Rak, A., and Alexandrov, K.** (2005). The structural and mechanistic

- basis for recycling of Rab proteins between membrane compartments. *Cell Mol. Life Sci.* **62**, 1657-1670.
- Grant, B.D., and Donaldson, J.G.** (2009). Pathways and mechanisms of endocytic recycling. *Nat. Rev. Mol. Cell Biol.* **10**, 597-608.
- Grosshans, B.L., Ortiz, D., and Novick, P.** (2006). Rabs and their effectors: Achieving specificity in membrane traffic. *Proc. Natl. Acad. of Sci. USA* **103**, 11821-11827.
- Haas, T.J., Sliwinski, M.K., Martinez, D.E., Preuss, M., Ebine, K., Ueda, T., Nielsen, E., Odorizzi, G., and Otegui, M.S.** (2007). The Arabidopsis AAA ATPase SKD1 is involved in multivesicular endosome function and interacts with its positive regulator LYST-INTERACTING PROTEIN5. *Plant Cell* **19**, 1295-1312.
- Hsu, V.W., and Prekeris, R.** (2010). Transport at the recycling endosome. *Curr. Opin. Cell Biol.* **22**, 528-534.
- Jaillais, Y., Fobis-Loisy, I., Miège, C., and Gaude, T.** (2007). Evidence for a sorting endosome in Arabidopsis root cells. *Plant J.* **53**, 237-247.
- Jean, S., and Kiger, A.A.** (2012). Coordination between RAB GTPase and phosphoinositide regulation and functions. *Nat. Rev. Mol. Cell Biol.* **13**, 463-470.
- Jolliffe, N.A., Craddock, C.P., and Frigerio, L.** (2005). Pathways for protein transport to seed storage vacuoles. *Biochem. Soc. Trans.* **33**, 1016-1018.
- Kang, B.H., Nielsen, E., Preuss, M.L., Mastronarde, D., and Staehelin, L.A.** (2011). Electron tomography of RabA4b- and PI-4Kbeta1-labeled trans Golgi network compartments in Arabidopsis. *Traffic* **12**, 313-329.
- Kirchhelle, C., Chow, C.M., Foucart, C., Neto, H., Stierhof, Y.D., Kalde, M., Walton, C., Fricker, M., Smith, R.S., Jérusalem, A., Irani, N., and Moore, I.** (2016). The specification of geometric edges by a plant Rab GTPase is an essential cell-patterning principle during organogenesis in Arabidopsis. *Dev. Cell* **36**, 386-400.

- Kotzer, A.M., Brandizzi, F., Neumann, U., Paris, N., Moore, I., and Hawes, C.** (2004). AtRabF2b (Ara7) acts on the vacuolar trafficking pathway in tobacco leaf epidermal cells. *J. Cell Sci.* **117**, 6377-6389.
- Lam, S.K., Siu, C.L., Hillmer, S., Jang, S., An, G., Robinson, D.G., and Jiang, L.** (2007). Rice SCAMP1 defines clathrin-coated, *trans*-golgi-located tubular-vesicular structures as an early endosome in tobacco BY-2 cells. *Plant Cell* **19**, 296-319.
- Lemmon, M.A.** (2008). Membrane recognition by phospholipid-binding domains. *Nat. Rev. Mol. Cell Biol.* **9**, 99-111.
- Li, L., Shimada, T., Takahashi, H., Ueda, H., Fukao, Y., Kondo, M., Nishimura, M., and Hara-Nishimura, I.** (2006). MAIGO2 is involved in exit of seed storage proteins from the endoplasmic reticulum in *Arabidopsis thaliana*. *Plant Cell* **18**, 3535-3547.
- Lupas, A., Van Dyke, M., and Stock, J.** (1991). Predicting coiled coils from protein sequences. *Science* **252**, 1162-1164.
- Lycett, G.** (2008). The role of Rab GTPases in cell wall metabolism. *J. Exp. Bot.* **59**, 4061-4074.
- Matsuoka, K., Bassham, D.C., Raikhel, N.V., and Nakamura, K.** (1995). Different sensitivity to wortmannin of two vacuolar sorting signals indicates the presence of distinct sorting machineries in tobacco cells. *J. Cell Biol.* **130**, 1307-1318.
- Miaczynska, M., Christoforidis, S., Giner, A., Shevchenko, A., Uttenweiler-Joseph, S., Habermann, B., Wilm, M., Parton, R.G., and Zerial, M.** (2004). APPL proteins link Rab5 to nuclear signal transduction via an endosomal compartment. *Cell* **116**, 445-456.
- Miao, Y., Li, K.Y., Li, H.Y., Yao, X., and Jiang, L.** (2008). The vacuolar transport of aleurain-GFP and 2S albumin-GFP fusions is mediated by the same pre-vacuolar compartments in tobacco BY-2 and *Arabidopsis* suspension cultured cells. *Plant J.* **56**, 824-839.

- Mizuno-Yamasaki, E., Rivera-Molina, F., and Novick, P.** (2012). GTPase networks in membrane traffic. *Annu. Rev. Biochem.* **81**, 637-659.
- Nakagawa, T., Kurose, T., Hino, T., Tanaka, K., Kawamukai, M., Niwa, Y., Toyooka, K., Matsuoka, K., Jinbo, T., and Kimura, T.** (2007). Development of series of gateway binary vectors, pGWBs, for realizing efficient construction of fusion genes for plant transformation. *J. Biosci. Bioeng.* **104**, 34-41.
- Nielsen, E., Cheung, A.Y., and Ueda, T.** (2008). The regulatory RAB and ARF GTPases for vesicular trafficking. *Plant Physiol.* **147**, 1516-1526.
- Nielsen, E., Christoforidis, S., Uttenweiler-Joseph, S., Miaczynska, M., Dewitte, F., Wilm, M., Hoflack, B., and Zerial, M.** (2000). Rabenosyn-5, a novel Rab5 effector, is complexed with hVPS45 and recruited to endosomes through a FYVE finger domain. *J. Cell Biol.* **151**, 601-612.
- Niemes, S., Langhans, M., Viotti, C., Scheuring, D., San Wan Yan, M., Jiang, L., Hillmer, S., Robinson, D.G., and Pimpl, P.** (2010). Retromer recycles vacuolar sorting receptors from the *trans*-Golgi network. *Plant J.* **61**, 107-121.
- Nishizawa, K., Maruyama, N., Satoh, R., Fuchikami, Y., Higasa, T., and Utsumi, S.** (2003). A C-terminal sequence of soybean beta-conglycinin alpha' subunit acts as a vacuolar sorting determinant in seed cells. *Plant J.* **34**, 647-659.
- Pedrazzini, E., Komarova, N.Y., Rentsch, D., and Vitale, A.** (2013). Traffic routes and signals for the tonoplast. *Traffic* **14**, 622-628.
- Pourcher, M., Santambrogio, M., Thazar, N., Thierry, A.M., Fobis-Loisy, I., Miège, C., Jaillais, Y., and Gaude, T.** (2010). Analyses of sorting nexins reveal distinct retromer-subcomplex functions in development and protein sorting in *Arabidopsis thaliana*. *Plant Cell* **22**, 3980-3991.
- Preuss, M.L.** (2006). A role for the RabA4b effector protein PI-4Kbeta1 in polarized expansion of root hair cells in *Arabidopsis thaliana*. *J. Cell Biol.* **172**, 991-998.
- Preuss, M.L., Serna, J., Falbel, T.G., Bednarek, S.Y., and Nielsen, E.** (2004). The *Arabidopsis* Rab GTPase RabA4b localizes to the tips of growing root hair cells.

Plant Cell **16**, 1589-1603.

Reguera, M., Bassil, E., Tajima, H., Wimmer, M., Chanoca, A., Otegui, M.S., Paris, N., and Blumwald, E. (2015). pH regulation by NHX-type antiporters is required for receptor-mediated protein trafficking to the vacuole in *Arabidopsis*. Plant Cell **27**, 1200-1217.

Ren, Y., Wang, Y., Liu, F., Zhou, K., Ding, Y., Zhou, F., Wang, Y., Liu, K., Gan, L., Ma, W., Han, X., Zhang, X., Guo, X., Wu, F., Cheng, Z., Wang, J., Lei, C., Lin, Q., Jiang, L., Wu, C., Bao, Y., Wang, H., and Wan, J. (2014). *GLUTELIN PRECURSOR ACCUMULATION3* encodes a regulator of post-Golgi vesicular traffic essential for vacuolar protein sorting in rice endosperm. Plant Cell **26**, 410-425.

Reyes, F.C., Buono, R., and Otegui, M.S. (2011). Plant endosomal trafficking pathways. Curr. Opin. Plant Biol. **14**, 666-673.

Saito, C., and Ueda, T. (2009). Chapter 4 Functions of RAB and SNARE proteins in plant life. Int. Rev. Cell Mol. Biol. **274**, 183-233.

Scheuring, D., Viotti, C., Kruger, F., Kunzl, F., Sturm, S., Bubeck, J., Hillmer, S., Frigerio, L., Robinson, D.G., Pimpl, P., and Schumacher, K. (2011). Multivesicular bodies mature from the *trans*-Golgi network/early endosome in *Arabidopsis*. Plant Cell **23**, 3463-3481.

Schnatwinkel, C., Christoforidis, S., Lindsay, M.R., Uttenweiler-Joseph, S., Wilm, M., Parton, R.G., and Zerial, M. (2004). The Rab5 effector Rabankyrin-5 regulates and coordinates different endocytic mechanisms. PLoS Biol. **2**, E261.

Seabra, M.C., and Wasmeier, C. (2004). Controlling the location and activation of Rab GTPases. Curr. Opin. Cell Biol. **16**, 451-457.

Shimada, T. (2003a). Vacuolar processing enzymes are essential for proper processing of seed storage proteins in *Arabidopsis thaliana*. J. Biol. Chem. **278**, 32292-32299.

Shimada, T. (2006). AtVPS29, a putative component of a retromer complex, is required

- for the efficient sorting of seed storage proteins. *Plant Cell Physiol.* **47**, 1187-1194.
- Shimada, T., Fuji, K., Tamura, K., Kondo, M., Nishimura, M., and Hara-Nishimura, I.** (2003b). Vacuolar sorting receptor for seed storage proteins in *Arabidopsis thaliana*. *Proc. Natl. Acad. of Sci. USA* **100**, 16095-16100.
- Shin, H.W., Hayashi, M., Christoforidis, S., Lacas-Gervais, S., Hoepfner, S., Wenk, M.R., Modregger, J., Uttenweiler-Joseph, S., Wilm, M., Nystuen, A., Frankel, W.N., Solimena, M., De Camilli, P., and Zerial, M.** (2005). An enzymatic cascade of Rab5 effectors regulates phosphoinositide turnover in the endocytic pathway. *J. Cell Biol.* **170**, 607-618.
- Simon, M.L., Platre, M.P., Assil, S., van Wijk, R., Chen, W.Y., Chory, J., Dreux, M., Munnik, T., and Jaillais, Y.** (2014). A multi-colour/multi-affinity marker set to visualize phosphoinositide dynamics in *Arabidopsis*. *Plant J.* **77**, 322-337.
- Simonsen, A., Lippe, R., Christoforidis, S., Gaullier, J.M., Brech, A., Callaghan, J., Toh, B.H., Murphy, C., Zerial, M., and Stenmark, H.** (1998). EEA1 links PI(3)K function to Rab5 regulation of endosome fusion. *Nature* **394**, 494-498.
- Singh, M.K., Kru"ger, F., Beckmann, H., Brumm, S., Vermeer, J.E.M., Munnik, T., Mayer, U., Stierhof, Y.-D., Grefen, C., Schumacher, K., and Ju"rgens, G.** (2014). Protein delivery to vacuole requires SAND protein-dependent RabGTPase conversion. *Curr. Biol.* **24**, 1383-1389.
- Shirakawa, M., Ueda, H., Koumoto, Y., Fuji, K., Nishiyama, C., Kohchi, T., Hara-Nishimura, I., and Shimada, T.** (2014). CONTINUOUS VASCULAR RING (COV1) is a *trans*-Golgi network-localized membrane protein required for Golgi morphology and vacuolar protein sorting. *Plant Cell Physiol.* **55**, 764-772.
- Sohn, E.J., Kim, E.S., Zhao, M., Kim, S.J., Kim, H., Kim, Y.W., Lee, Y.J., Hillmer, S., Sohn, U., Jiang, L., and Hwang, I.** (2003). Rha1, an *Arabidopsis* Rab5 homolog, plays a critical role in the vacuolar trafficking of soluble cargo

- proteins. *Plant Cell* **15**, 1057-1070.
- Somsel Rodman, J., and Wandinger-Ness, A.** (2000). Rab GTPases coordinate endocytosis. *J. Cell Sci.* **113 Pt 2**, 183-192.
- Stenmark, H.** (2009). Rab GTPases as coordinators of vesicle traffic. *Nat. Rev. Mol. Cell Biol.* **10**, 513-525.
- Stenmark, H., Vitale, G., Ullrich, O., and Zerial, M.** (1995). Rabaptin-5 is a direct effector of the small GTPase Rab5 in endocytic membrane fusion. *Cell* **83**, 423-432.
- Stierhof, Y.D., and El Kasmi, F.** (2010). Strategies to improve the antigenicity, ultrastructure preservation and visibility of trafficking compartments in *Arabidopsis* tissue. *Eur. J. Cell Biol.* **89**, 285-297.
- Sunada, M., Goh, T., Ueda, T., and Nakano, A.** (2016). Functional analyses of the plant-specific C-terminal region of VPS9a: the activating factor for RAB5 in *Arabidopsis thaliana*. *J. Plant Res.* **129**, 93-102.
- Szumanski, A.L., and Nielsen, E.** (2009). The Rab GTPase RabA4d regulates pollen tube tip growth in *Arabidopsis thaliana*. *Plant Cell* **21**, 526-544.
- Takahashi, H., Tamura, K., Takagi, J., Koumoto, Y., Hara-Nishimura, I., and Shimada, T.** (2010). MAG4/Atp115 is a Golgi-localized tethering factor that mediates efficient anterograde transport in *Arabidopsis*. *Plant Cell Physiol.* **51**, 1777-1787.
- Tamura, K., Takahashi, H., Kunieda, T., Fuji, K., Shimada, T., and Hara-Nishimura, I.** (2007). *Arabidopsis* KAM2/GRV2 is required for proper endosome formation and functions in vacuolar sorting and determination of the embryo growth axis. *Plant Cell* **19**, 320-332.
- Teh, O.K., Hatsugai, N., Tamura, K., Fuji, K., Tabata, R., Yamaguchi, K., Shingenobu, S., Yamada, M., Hasebe, M., Sawa, S., Shimada, T., and Hara-Nishimura, I.** (2015). BEACH-domain proteins act together in a cascade to mediate vacuolar protein trafficking and disease resistance in *Arabidopsis*.

- Mol. Plant **8**, 389-398.
- Tian, G.W.** (2004). High-throughput fluorescent tagging of full-length Arabidopsis gene products in planta. *Plant Physiol.* **135**, 25-38.
- Ueda, T., Yamaguchi, M., Uchimiya, H., and Nakano, A.** (2001). Ara6, a plant-unique novel type Rab GTPase, functions in the endocytic pathway of *Arabidopsis thaliana*. *EMBO J.* **20**, 4730-4741.
- Ueda, T., Uemura, T., Sato, M.H., and Nakano, A.** (2004). Functional differentiation of endosomes in Arabidopsis cells. *Plant J.* **40**, 783-789.
- Uejima, T., Ihara, K., Goh, T., Ito, E., Sunada, M., Ueda, T., Nakano, A., and Wakatsuki, S.** (2010). GDP-bound and nucleotide-free intermediates of the guanine nucleotide exchange in the Rab5-Vps9 System. *J. Biol. Chem.* **285**, 36689-36697.
- Uejima, T., Ihara, K., Sunada, M., Kawasaki, M., Ueda, T., Kato, R., Nakano, A., and Wakatsuki, S.** (2013). Direct metal recognition by guanine nucleotide-exchange factor in the initial step of the exchange reaction. *Acta Crystallogr. D Biol. Crystallogr.* **69**, 345-351.
- van Leeuwen, W., Ökrész, L., Bögre, L., and Munnik, T.** (2004). Learning the lipid language of plant signalling. *Trends Plant Sci.* **9**, 378-384.
- Vermeer, J.E.M., van Leeuwen, W., Tobeña-Santamaria, R., Laxalt, A.M., Jones, D.R., Divecha, N., Gadella, T.W.J., and Munnik, T.** (2006). Visualization of PtdIns3P dynamics in living plant cells. *Plant J.* **47**, 687-700.
- Viotti, C., Bubeck, J., Stierhof, Y.D., Krebs, M., Langhans, M., van den Berg, W., van Dongen, W., Richter, S., Geldner, N., Takano, J., Jurgens, G., de Vries, S.C., Robinson, D.G., and Schumacher, K.** (2010). Endocytic and secretory traffic in Arabidopsis merge in the *trans*-Golgi network/early endosome, an independent and highly dynamic organelle. *Plant Cell* **22**, 1344-1357.
- Vitale, A., and Hinz, G.** (2005). Sorting of proteins to storage vacuoles: how many mechanisms? *Trends Plant Sci.* **10**, 316-323.

- Wen, L., Fukuda, M., Sunada, M., Ishino, S., Ishino, Y., Okita, T.W., Ogawa, M., Ueda, T., and Kumamaru, T.** (2015). Guanine nucleotide exchange factor 2 for Rab5 proteins coordinated with GLUP6/GEF regulates the intracellular transport of the proglutelin from the Golgi apparatus to the protein storage vacuole in rice endosperm. *J. Exp. Bot.* **66**, 6137-6147.
- Winter, D., Vinegar, B., Nahal, H., Ammar, R., Wilson, G.V., and Provart, N.J.** (2007). An "Electronic Fluorescent Pictograph" browser for exploring and analyzing large-scale biological data sets. *PLoS One* **2**, e718.
- Woollard, A.A.D., and Moore, I.** (2008). The functions of Rab GTPases in plant membrane traffic. *Curr. Opin. Plant Biol.* **11**, 610-619.
- Yamazaki, M., Shimada, T., Takahashi, H., Tamura, K., Kondo, M., Nishimura, M., and Hara-Nishimura, I.** (2007). Arabidopsis VPS35, a retromer component, is required for vacuolar protein sorting and involved in plant growth and leaf senescence. *Plant Cell Physiol.* **49**, 142-156.
- Zerial, M., and McBride, H.** (2001). Rab proteins as membrane organizers. *Nat. Rev. Mol. Cell Biol.* **2**, 107-117.